Title: Overlapping Central Clock Network Circuitry Regulates Circadian Feeding and Activity Rhythms in *Drosophila*

Running Title: Overlapping Circuitry for Circadian Feeding and Activity Rhythms

Author Names and Affiliation: Sumit Saurabh[1], Ruth J. Meier[1], Liliya M. Pireva[1], Rabab A. Mirza[1] and Daniel J. Cavanaugh[1]

1. Department of Biology, Loyola University Chicago, 60660

Corresponding Author:

Daniel J. Cavanaugh

Department of Biology

Loyola University Chicago

1050 W. Sheridan Rd.

Chicago, IL 60660 Email: dcavanaugh1@luc.edu

Acknowledgements: We thank David Anderson, Tom Clandinin, Fumika Hamada, Paul Hardin, Michael Rosbash, Gerry Rubin, Amita Sehgal, Orie Shafer, Mimi Shirasu-Hiza, and the Bloomington *Drosophila* Stock Center for fly stocks and Amita Sehgal for antisera.

Funding: The authors disclosed receipt of the following financial support for the research, authorship, and/or publication of this article: This work was supported by the Division of Integrative Organismal Systems of the National Science Foundation, CAREER Award 1942167 to D.J.C.

Declaration of Conflicting Interests: The authors declare that there is no conflict of interest.

Abstract

The circadian system coordinates multiple behavioral outputs to ensure proper temporal organization. Timing information underlying circadian regulation of behavior depends on a molecular circadian clock that operates within clock neurons in the brain. In *Drosophila* and other organisms, clock neurons can be divided into several molecularly and functionally discrete subpopulations that form an interconnected central clock network. It is unknown how circadian signals are coherently generated by the clock network and transmitted across output circuits that connect clock cells to downstream neurons that regulate behavior. Here we have exhaustively investigated the contribution of clock neuron subsets to the control of two prominent behavioral outputs in *Drosophila*: locomotor activity and feeding. We have used cell-specific manipulations to eliminate molecular clock function or induce electrical silencing either broadly throughout the clock network or in specific subpopulations. We find that clock cell manipulations produce similar changes in locomotor activity and feeding, suggesting that overlapping central clock circuitry regulates these distinct behavioral outputs. Interestingly, the magnitude and nature of the effects depend on the clock subset targeted. Lateral clock neuron manipulations profoundly degrade the rhythmicity of feeding and activity. In contrast, dorsal clock neuron manipulations only subtly affect rhythmicity but produce pronounced changes in the distribution of activity and feeding across the day. These experiments expand our knowledge of clock regulation of activity rhythms and offer the first extensive characterization of central clock control of feeding rhythms. Despite similar effects of central clock cell disruptions on activity and feeding, we find that manipulations that prevent functional signalling in an identified output circuit preferentially degrade locomotor activity rhythms, leaving feeding rhythms relatively intact. This demonstrates that activity and feeding are indeed dissociable behaviors, and furthermore suggests that differential circadian control of these behaviors diverges in output circuits downstream of the clock network.

Key Words

Drosophila, circadian, clock network, feeding, locomotor activity

Introduction

Organisms use a genetically-determined circadian timing system to align physiological processes with the 24-hr environmental cycles produced by the Earth's daily rotation on its axis (Allada & Chung, 2010). At its core, the circadian system relies on the function of an intrinsic, cell-autonomous molecular clock that is present in central clock cells in the brain as well as most peripheral tissues. Critically, this imposes circadian organization across tissues, allowing organisms to compartmentalize and optimize their metabolic and behavioral outputs to maximize fitness (Panda, 2016; Patke et al., 2020; Vaze & Sharma, 2013). The importance of the circadian system for organismal health is evidenced by the severe consequences associated with circadian disruption or misalignment, including increased risk of cancer, neurological diseases, metabolic dysfunction and obesity (Logan & McClung, 2019; Nassan & Videnovic, 2022; Potter et al., 2016; Roenneberg & Merrow, 2016; Sletten et al., 2020).

Much of our knowledge of circadian clocks derives from studies initially conducted in the fruit fly, *Drosophila melanogaster* (Tataroglu & Emery, 2014). The *Drosophila* molecular clock functions as a transcriptional-translational feedback loop that centers around four core clock genes - *period* (*per*), *timeless* (*tim*), *clock* (*Clk*), and *cycle* (*cyc*) - and their protein products. CLK and CYC proteins are transcription factors that drive expression of the *per* and *tim* genes. PER and TIM proteins build up during the day and form heterodimer complexes that translocate to the nucleus at night to suppress CLK/CYC-mediated transcription. PER and TIM are then degraded, relieving their repression of CLK and CYC and initiating a new round of transcription. This process takes ~24 hrs to complete (Allada & Chung, 2010; Patke et al., 2020). In addition to *per* and *tim*, CLK and CYC produce rhythmic expression of many additional clock-controlled genes,

ultimately resulting in circadian modulation of tissue-specific function (Patke et al., 2020). Notably, the molecular clock mechanism and major clock genes are conserved across species.

The molecular circadian clock operates in a dedicated group of ~150 interconnected neurons (75 per hemisphere) in the fly brain, which together comprise the central clock network. These neurons have been divided into 7 major subsets that occupy distinct anatomical locations inside the central brain: the ventral lateral neurons (LNvs), dorsal lateral neurons (LNds), lateral posterior neurons (LPNs), and three groups of dorsal neurons (DN1s, DN2s and DN3s) (Allada & Chung, 2010; King & Sehgal, 2020). Recent transcriptomic analysis suggests that these can be further subdivided into at least 17 subsets based on differential gene expression (Ma et al., 2021). Studies conducted on clock cells in the suprachiasmatic nucleus (SCN), the mammalian equivalent of the *Drosophila* clock neurons, suggest a similar organization with multiple, molecularly distinct populations of interconnected neurons that together generate rhythmic behavioral outputs (Hastings et al., 2018; Wen et al., 2020; P. Xu et al., 2021).

Given its relatively compact nervous system and a plethora of experimental and genetic tools, *Drosophila* has become an important model for exploring the intricate workings of the clock neuronal network and its downstream targets in the regulation of behavior. To date, most circadian research in *Drosophila* has focused on locomotor activity rhythms as a behavioral endpoint. Initial studies identified a particularly important role for the lateral clock neurons (LNvs and LNds) in generating circadian locomotor activity rhythms and maintaining them under constant environmental conditions (Grima et al., 2004; Helfrich-Förster, 1998; Picot et al., 2007; Renn et al., 1999; Stoleru et al., 2004). In contrast, dorsal clock neurons (DN1s, DN2s and DN3s) have been assigned a more modulatory function (Bulthuis et al., 2019; Díaz et al., 2019; Fujiwara et al., 2018; Guo et al., 2016; Nettnin et al., 2021; L. Zhang et al., 2010; Y. Zhang et al., 2010). Despite this, it is clear that coherent locomotor activity rhythms require coordinated

output from multiple clock cell populations (Beckwith & Ceriani, 2015; Bulthuis et al., 2019; Chatterjee et al., 2018; Delventhal et al., 2019; Schlichting et al., 2019). Thus, circadian activity rhythms derive from interactions across most of the clock network.

Several other behaviors in addition to locomotor activity have been shown to be under circadian control in adult *Drosophila*, including courtship and mating (Fujii et al., 2007; Sakai & Ishida, 2001), egg laying (Howlader et al., 2006), temperature preference (Kaneko et al., 2012), grooming (Qiao et al., 2018), and feeding (K. Xu et al., 2008). An important question is how the central brain clock coordinates these distinct behavioral outputs, and in particular, whether they rely on shared versus distinct central clock network circuitry. To that end, we and others have begun to delineate the circuit mechanisms underlying circadian control of feeding behavior. Circadian feeding rhythms are abrogated following manipulations that electrically silence or eliminate molecular clock function selectively in LNv clock cells (Barber et al., 2021; Fulgham et al., 2021), pointing to an essential contribution from this central clock population. As LNv cells also critically contribute to locomotor activity rhythms, these results indicate at least some overlap in the cellular control of feeding and locomotor activity rhythms. Nevertheless, manipulations of circadian output cell populations demonstrate dissociable circadian regulation of these behaviors, indicating the presence of distinct control mechanisms (King et al., 2017).

Here we sought to further clarify the role of different clock network subsets as well as downstream neuronal targets in the generation of circadian feeding rhythms, and to compare this to circuit control of locomotor activity rhythms. We monitored feeding and locomotor activity in flies in which we targeted distinct clock network subsets with transgenes that either disrupt molecular clock function or induce neuronal silencing. We find that free-running feeding rhythms require molecular clock function within multiple individual clock cell populations, and furthermore that the severity of the effect varies according to the cell population targeted. These results

parallel those observed when using locomotor activity as a behavioral endpoint, suggesting that circadian control of these two distinct behavioral outputs diverges in downstream circadian output cells rather than in cells of the core clock network. In line with this possibility, we confirm previous results demonstrating that elimination of the DH44-R1 receptor, which is expressed in neurons that comprise part of a circadian output circuit for control of locomotor activity (King et al., 2017), preferentially degrades locomotor activity rhythms while producing comparatively minor effects on feeding rhythms. Our data support a model in which divergent circadian control over distinct behavioral outputs arises from clock network connections with separable output circuits.

Materials and Methods

Fly Lines

All fly stocks were raised in narrow polystyrene vials (Fisher Scientific) under 12:12 light-dark (LD) cycles. Flies were provided a cornmeal-molasses medium consisting of (per L of food): 1L deionized water, 64.7 g yellow cornmeal, 27.1 g dry active granular yeast, 8.0 grams 80-100 mesh agar, 90 g unsulphured molasses and supplemented with 4.4 mL propionic acid and 2.0 g Tegosept to prevent contamination. Clk856-GAL4 (FBti0217049) (Gummadova et al., 2009) was provided by O. Shafer. Pdf-GAL80.96A (II) (FBti0074329) and Pdf-GAL80 (III) (Stoleru et al., 2004) were provided by M. Rosbash. SS00681-sGAL4 (w; R65B09-p65ADZp in attP40; R18D09-ZpGdbd in attP2), MB122B-sGAL4 (w; R12G04-p65ADZp in attP40/CyO::Tb-RFP; R18D09-ZpGdbd in attP2), SS00781-sGAL4 (w; R20G07-p65ADZp in attP40; R18H11-ZpGdbd in attP2) and SS00367-sGAL4 (w; R67F03-p65ADZp in attP40/CyO; R10G01-ZpGdbd in attP2) were provided by H. Dionne, A. Nern and G. Rubin. Clk4.1M-GAL4 (FBti0212837) (L. Zhang et al., 2010) was provided by P. Hardin. InSITE911-GAL4 (FBti0181438) (Gohl et al., 2011) was provided by T. Clandinin. LNd-GAL4 (Bulthuis et al., 2019) consists of DvPdf-GAL4 (FBal0279528) (Bahn et al., 2009), provided by M. Rosbash, R78G02-GAL4 (FBti0191901),

provided by the Bloomington *Drosophila* Stock Center (BDSC) and two copies of Pdf-GAL80; one each on the second and third chromosome. Clk9M-GAL4;Pdf-GAL80 (Kaneko et al., 2012) was provided by F. Hamada. UAS-gRNA-*per*, UAS-gRNA-*tim*, and UAS-gRNA-*acp* (Delventhal et al., 2019) were provided by M. Shirasu-Hiza. UAS-Cas9.P2 (FBti0166499) was provided by the BDSC. To simplify nomenclature, we refer to flies in which a GAL4 driver was used to express both the gene-specific gRNA and Cas9 as GAL4>*acp*^{CRISPR}, GAL4>*per*^{CRISPR}, and GAL4>*tim*^{CRISPR}. UAS>eGFP::Kir2.1-stop>mCherry and UAS>mCherry-stop>eGFP::Kir2.1 (Watanabe et al., 2017) were provided by D. Anderson. To simplify nomenclature, we refer to flies in which a GAL4 driver was used to express these constructs as GAL4>mCherry and GAL4>Kir2.1^{eGFP}. UAS-mCD8::GFP, Iso31 (Ryder et al., 2004) and *Dh44-R1*^{dsred} (King et al., 2017) were provided by A. Sehgal.

Dh44-R1^{dsred} mutants were outcrossed 7x to the Iso31 background. GAL4 and UAS lines used for CRISPR and Kir2.1 experiments were not outcrossed, but our experimental design ensured that genetic background was held constant across corresponding control and experimental flies. For example, *per*^{CRISPR}, *tim*^{CRISPR} and *acp*^{CRISPR} effector lines all contain UAS-guide RNA and UAS-Cas9.P2 constructs that are inserted into the same genomic location in flies of the same genetic background. These effectors were crossed to identical GAL4 driver lines. Thus, experimental and control flies always consist of the same mixed genetic background with an equal number of transgenic insertions in the same genomic locations. This is also true of our silencing experiments, in which GAL4 is used to drive effector constructs (UAS>eGFP::Kir2.1-stop>mCherry in experimental flies and UAS>mCherry-stop>eGFP::Kir2.1 in control flies) that are inserted into the same genomic location in flies of the same genetic background.

Locomotor Activity Monitoring and Analysis

Drosophila males, aged 7-10 d, were entrained to a 12:12 LD cycle prior to experiments. Flies were anesthetized using CO_2 and individually housed in glass behavior tubes (Trikinetics Inc., Waltham, MA) containing a solid 5% sucrose and 2% agar food solution at one end. The tubes were then loaded into *Drosophila* Activity Monitors (DAM2, Trikinetics Inc., Waltham, MA) for locomotor activity monitoring for 6 d at 25°C under conditions of constant darkness (DD). The DAM system infers locomotor activity based on the breaking of an infrared beam that transects the middle of each behavior tube. DAM beam break data were summed into 30 min bins for data analysis. Data from the first 12 hrs of the experiment were excluded from data analysis to allow for acclimation to the behavioral monitoring apparatus. Locomotor activity rhythm period and power were determined by Lomb-Scargle periodogram analysis using ClockLab software (Actimetrics, Wilmette IL). The Lomb-Scargle “Amplitude” value at the dominant period is reported as a measure of rhythm strength (power). Flies with Lomb-Scargle “Amplitude” value that exceeded the “Probability” value at a significance level of $p < 0.01$ were deemed rhythmic. Flies that were found to have died during the experiment based on visual inspection of data were excluded from analysis. All flies that survived through the entire one-week monitoring period were included in determining the mean locomotor activity rhythm power. Only rhythmic flies were included in calculation of mean period. To calculate total activity, we determined the mean number of DAM beam breaks per minute over the course of the 6-day experiment for each individual fly.

Feeding Monitoring and Analysis

Male flies were aged and entrained as in DAM assays. Flies were aspirated into individual wells of Fly Liquid-Food Interaction Counter (FLIC) monitors (Sable Systems) that were fitted with food reservoirs to maintain adequate food levels during long-term monitoring. To allow for acclimation, recording of feeding behavior began 12 hrs after flies were initially loaded into FLIC monitors, and feeding monitoring was then conducted over 6 days in DD at 25°C. Liquid food

solution consisted of a 10% sugar solution with 45 mg/L $MgCl_2$ for increased circuit conductance. The FLIC monitor detects and records fly interactions with food via a conductive metal pad that surrounds the food and connects to a circuit board. A control unit receives voltage signals from the monitor every 200 milliseconds that are generated when a fly stands on the metal pad and interacts with the food, completing a circuit. Raw data from FLIC experiments were processed using R code (Pletcher Lab) (Ro et al., 2014) to extract feeding events, which we defined as times when the signal amplitude 1) exceeded the baseline readings by 5 mV for a minimum of 4 consecutive 200 ms recording periods, and 2) at some point during the event, achieved a 15 mV feeding threshold above baseline readings. Feeding events therefore have a minimum duration of 800 ms and are made up of multiple individual 200 ms feeding interactions, termed “licks”. For rhythm analysis, we summed lick data for individual flies into 30-min bins. Feeding rhythm period and power were determined through the ClockLab analysis software as described for locomotor activity rhythms. Dead flies or flies with poor signal were removed from analysis after visual inspection of data. To determine total feeding, we calculated the total duration of feeding events over the 6 d for each individual fly by multiplying the total number of licks by 200 ms, and then converting this to mean minutes of feeding per day.

Generation of average day eduction plots

To visualize the temporal organization of locomotor activity and feeding, we created average day eduction plots. We first normalized individual fly locomotor activity or feeding data for each fly by dividing the value from each 30 min bin by the mean activity or feeding per 30 min across the 6d experiment. We then determined the mean normalized activity or feeding for each 30 min bin by averaging the value at that timepoint for each of the 6 d of recording. Finally, we averaged these values across all flies of a given genotype.

Immunohistochemical staining and quantification

7 d old adult males were anesthetized with CO_2 at lights-on time (ZT0) and transferred to 100% ethanol for 1 min, then rinsed briefly in phosphate buffered saline with 0.1% Triton-X (PBST) before dissection in PBST. Harvested brains were fixed in 4% paraformaldehyde for 20-40 min, blocked for 60 min in 5% normal donkey serum in PBST (NDST) and incubated for 24 hrs in primary antibodies diluted in NDST. Primary antibodies were rabbit anti-GFP 1:1000 (Invitrogen A10262), guinea pig anti-PER 1:1000 (UPR 1140; gift of A. Sehgal), and mouse anti-PDF 1:1000 (Developmental Studies Hybridoma Bank PDFC7; generated by J. Blau). Brains were then washed 3x15 mins in PBST, incubated for 24 hrs in secondary antibodies diluted in NDST, washed 3x15 min PBST, cleared for 5 min in 50% glycerol in PBST, and mounted with Vectashield (Vector Labs). Secondary antibodies were FITC donkey anti-rabbit 1:1000 (Jackson 711-095-152), Cy3 donkey anti-guinea pig 1:1000 (Jackson 706-165-148) and Cy5 donkey anti-mouse 1:1000 (Jackson 715-175-151). Immunolabeled brains were visualized with a FLUOVIEW 1000 confocal microscope (Olympus).

To monitor adult brain expression patterns of the different GAL4 lines (Figure S1), we drove expression of mCD8::GFP. We kept image capture settings constant during imaging of all GAL4 lines but applied different brightness adjustment for each image (uniform across all pixels within the image). Thus, GFP intensity does not reflect strength of GAL4 activity, but rather is optimized for each image to best identify GAL4-expressing cells. To confirm CRISPR-mediated molecular clock abrogation, we stained brains for PER expression. For each genotype, 7-11 brains were immunostained. For quantification, we manually counted the number of PER-positive nuclei in each clock neuronal subset (lLNVs, sLNvs, LNds, LPNs, DN1s and DN2s) in one brain hemisphere per fly. This qualitative assessment involved identifying cells in which PER immunosignal was clearly distinguishable from background staining in nearby brain regions. We used PDF staining and cell size to identify lLNv and sLNv neurons, and identified the other cell populations based on stereotypical anatomical position in the brain.

Statistical Data Analysis

Three or four experimental replicates were conducted for all behavioral experiments, and data were combined from all replicates for final analyses. For making comparisons across experiments and treatments, locomotor activity and feeding rhythm power data were normalized for each experimental replicate by dividing the power value for each fly by the mean power value of the experimental control group for that experiment. Data were then analyzed using GraphPad Prism 10 (GraphPad) software. For comparisons in experiments with 3 groups, Welch's ANOVA with Dunnett's T3 multiple comparisons test were used. For experiments consisting of 2 groups, Welch's t-test was used. For comparisons of PER staining, Kruskal-Wallace with Dunn's multiple comparisons test were used. p values of < 0.05 with respect to all relevant controls were deemed significant.

Results

Selective manipulation of central clock neuron subsets

We used the GAL4-UAS binary gene expression system (Brand & Perrimon, 1993) for selective manipulation of the different central clock subpopulations. We first validated a library of 10 GAL4 lines to confirm expression within cells of the central clock network (Figure S1). Notably, these GAL4 drivers allow us to target broad populations of clock cells (Clk856-GAL4; Figure S1A, Clk856-GAL4; Pdf-GAL80; Figure S1B), as well as most major subclasses including sLNvs (SS00681-sGAL4; Figure S1C), LNds (LNd-GAL4; Figure S1D, MB122B-sGAL4; Figure S1E), DN1s (InSITE911-GAL4; Figure S1F, Clk4.1-GAL4; Figure S1G, SS00781-sGAL4; Figure S1H), DN2s (Clk9M-GAL4; Pdf-GAL80; Figure S1I) and DN3s (SS00367-GAL4; Figure S1J). For many of these lines, GAL4 expression is exquisitely restricted to the cell population of interest.

To test the functional specificity of these GAL4 lines, we used them as part of a cell-specific CRISPR approach to selectively abrogate molecular clock function in clock neuron subsets (Delventhal et al., 2019). In this setup, CRISPR constructs targeting either the *per* or *tim* gene are expressed in a GAL4-dependent manner. To determine the efficacy of molecular clock disruption, we performed immunohistochemistry on fly brains and quantified the number of PER-positive nuclei in each clock neuronal subset (Figure 1). In general, these results were consistent with expectations and demonstrated effective elimination of PER protein from the appropriate neuronal populations. For example, we observed a near complete elimination of PER expression in the brains of Clk856>*per*^{CRISPR} flies, while PER was selectively removed from sLNvs when we used the sLNv-specific SS00681-sGAL4 line (Figure 1C, F-L; Table 1).

An exception to the fidelity of our approach occurred with GAL4 lines that simultaneously included a Pdf-GAL80 construct to delimit GAL4 activity. GAL80 prevents GAL4-mediated transcription; thus, use of the Pdf-GAL80 transgene should exclude GAL4 activity from the Pdf-expressing LNv clock cells. Though Pdf-GAL80 was sufficient to prevent membrane-tethered GFP expression in LNv neurons (Figure S1B, D and I), it was ineffective at suppressing CRISPR-mediated *per* excision in these cells. Thus, flies in which we drove *per*^{CRISPR} expression using Clk856-GAL4; Pdf-GAL80 to target non-LNv clock cells, LNd-GAL4 (which combines 2 GAL4 lines along with 2 copies of Pdf-GAL80; see methods; Bulthuis et al., 2019) to target LNds, and Clk9M-GAL4; Pdf-GAL80 to target DN2 clock cells retained PER protein expression in only ~1 to 2 of 4 sLNvs (Figure 1F; Table 1). Clk856;Pdf80>*per*^{CRISPR} and LNd>*per*^{CRISPR} flies also lacked PER expression in virtually all lLNvs (Figure 1H; Table 1). Because CRISPR effects are permanent once induced in a cell, these results suggest that Pdf-GAL80 turns on at a later developmental time point than GAL4 in these cells, resulting in CRISPR-mediated excision of the *per* gene that cannot be reversed by later GAL80 expression. We also found that in addition to the expected loss of PER in DN2s, Clk9M;Pdf80>*per*^{CRISPR} flies had a reduced number of

PER-expressing DN1 cells (Figure 1K; Table 1), indicative of transient GAL4 expression in this cell population.

Molecular clock abrogation in lateral clock neurons strongly disrupts feeding and activity rhythms

Having characterized the molecular consequences of CRISPR-mediated clock abrogation, we next used these flies to determine the requirement for cell-autonomous molecular clock function within central clock cells in the generation of circadian activity and feeding rhythms. In these experiments, we compared behavior of experimental flies in which *per*- or *tim*-targeting CRISPR constructs were selectively expressed in different clock cell groups to a control group of flies that expressed CRISPR constructs targeting the *Acp98AB* gene, which encodes for an accessory gland protein not involved in molecular clock function (Delventhal et al., 2019). We monitored activity and feeding behavior over 6 consecutive days using the DAM and FLIC (Ro et al., 2014) systems, respectively. To eliminate direct light effects on behavior and isolate the contribution of the endogenous circadian clock, we conducted these assays under DD conditions. This parallel assessment of the effects of the same genetic manipulations on locomotor activity and feeding rhythms allowed us to investigate whether distinct central clock network mechanisms regulate these two clock outputs.

We began by broadly disrupting molecular clock function using the Clk856-GAL4 line, which is expressed in the majority of brain clock cells, including neurons from all 7 major clock cell populations (Figure S1A) (Gummadova et al., 2009). Consistent with previous findings (Bulthuis et al., 2019; Schlichting et al., 2019), this manipulation abolished locomotor activity rhythms. Lomb-Scargle periodogram analysis showed that only a very small percentage of Clk856>*per*^{CRISPR} and Clk856>*tim*^{CRISPR} flies exhibited rhythmic locomotor activity (Table S1), resulting in a profound reduction in activity rhythm power (Figure 2A). This was associated with

a drastic change in the distribution of activity across the circadian day. In comparison to control flies, which showed the expected daily oscillation of locomotor activity during an average DD day, flies lacking *per* or *tim* in most central brain clock cells exhibited flat activity patterns with no temporal variation across the day (Figure 2F). Not surprisingly, CRISPR-mediated molecular clock elimination in central brain clock neurons also resulted in arrhythmic feeding behavior (Figure 2K and P), phenocopying the effect of global clock gene knockouts on this behavior (Barber et al., 2021; Fulgham et al., 2021; Ro et al., 2014; Seay & Thummel, 2011; K. Xu et al., 2008). These results confirm an essential contribution of brain clocks in the generation of feeding rhythms, as has been suggested previously (Barber et al., 2021; Fulgham et al., 2021).

LNv clock cells have a central role in maintaining circadian rhythms of locomotor activity in constant environmental conditions (Renn et al., 1999), and we recently showed that molecular clocks within these cells also critically regulate feeding rhythms, conferring pacemaker function in the determination of the period length of feeding rhythms (Fulgham et al., 2021). Here, we conducted additional tests to further assess the role of the LNvs in circadian behavior. To investigate whether molecular clock activity restricted to LNv cells is alone sufficient to drive activity and feeding rhythms, we combined Clk856-GAL4 with Pdf-GAL80, which should limit CRISPR targeting to non-LNv clock cells. This strongly degraded both feeding and locomotor activity rhythms (Figure 2B, G, L and Q). We note that the incomplete ability of Pdf-GAL80 to suppress CRISPR-mediated gene editing in sLNv and lLNv clock cells in this line (Figure 1B, F and H; Table 1) complicates interpretation of these behavioral results, as these flies lack molecular clock function in the majority of LNv clock cells.

In addition to assessing for the sufficiency of LNv clocks to drive rhythm behavior, we also tested for the necessity of LNv clocks through the use of SS00681-sGAL4 to eliminate molecular clock function exclusively in sLNv clock cells (Figure 1C, F-L; Table 1). This produced

a robust suppression of both feeding and locomotor activity rhythms (Figure 2C, H, M and R). This is consistent with our previous results using Pdf-GAL4 to target both small and large LNv subsets (Fulgham et al., 2021) and furthermore demonstrates that clock activity is specifically required in sLNvs for intact feeding rhythms. Despite a drastic reduction in locomotor and feeding rhythm power in flies in which the sLNvs (SS00681-sGAL4) or non-LNv clock cells (Clk856-GAL4;Pdf-GAL80) were selectively targeted for molecular clock elimination (Figure 2B, C, L and M), group mean activity plots demonstrate that oscillations in feeding and activity behavior are reduced but not eliminated in these flies (Figure 2G, H, Q and R). In line with this, more than half of these flies retained rhythmic activity and feeding (Table S1), though rhythm strength was clearly reduced compared to controls. This contrasts to manipulations of the entire clock network (with Clk856-GAL4), which completely eliminate rhythms (Figure 2F and P; Table S1), thereby indicating that intact molecular clock function within multiple, independent nodes of the clock network is able to partially sustain behavioral rhythms in the face of largescale molecular clock dysfunction.

We also tested the impact of molecular clock ablation in LNd clock neurons, another important clock network population for control of locomotor activity rhythms. For this, we used two different GAL4 lines: MB122B-sGAL4, which is expressed in 3 out of 6 LNd cells per brain hemisphere (Figure S1E), and LNd-GAL4, which is expressed in all 6 LNds (Figure S1D). Both GAL4 lines additionally label the Pdf-negative 5th sLNv. We observed that disrupting the clock in all LNd cells with LNd-GAL4 strongly reduced the strength of free-running feeding rhythms (Figure 2N). CRISPR-mediated clock gene disruption with MB122B-sGAL4 also produced a significant disruption of feeding rhythms, though this was muted compared to manipulations with LNd-GAL4 (Figure 2O and T). The differential effect size could derive from the fact that MB122B-sGAL4 incompletely labels the LNd population, or because of the residual loss of LNv clocks in the LNd-GAL4 line (Figure 1F and H). For both LNd-targeting GAL4 lines, we observed a

reduction in the strength of locomotor activity rhythms that largely paralleled the decrease in feeding rhythm strength (Figure 2D, E, I and J), although we note that the impact of molecular clock elimination in MB122B-sGAL4-expressing cells did not reach statistical significance across both *per* and *tim*-targeting CRISPR constructs (Figure 2E). The latter result raises the possibility that molecular clock elimination in MB122B-sGAL4-expressing clock cells may preferentially alter feeding behavior, which is also supported by group mean feeding and activity graphs. There was a significant alteration of the temporal pattern of feeding behavior in these flies characterized mainly by a shift peak feeding time in experimental flies (Figure 2T). In contrast, there was a much more subtle difference compared to controls in the distribution of locomotor activity across the day (Figure 2J).

Electrical silencing of lateral clock neurons strongly disrupts feeding and activity rhythms

In addition to molecular clock elimination, we conducted experiments in which we used the same GAL4 drivers to express the inhibitory Kir2.1 potassium channel, which hyperpolarizes neurons to effectively silence neuronal communication (Baines et al., 2001; Watanabe et al., 2017). Control flies expressed a GAL4-driven mCherry construct inserted into the same genomic location. With minor exceptions, we observed similar effects in these experiments as in those in which we drove *per* or *tim*-targeting CRISPR constructs. Thus, near-ubiquitous clock cell silencing in Clk856>Kir2.1^{eGFP} flies resulted in complete arrhythmicity for both feeding and locomotor behavior (Figure 3A, E, I and M; Table S2). Both behavioral rhythms were also substantially compromised in Clk856-GAL4; Pdf-GAL80>Kir2.1^{eGFP} flies, though, as was the case for our CRISPR experiments, some residual rhythmicity was retained in these flies such that they exhibited stronger circadian cycling as compared to flies in which all clock neurons were silenced (Figure 3B, F, J and N; Table S2). Because Kir2.1 requires ongoing activity for silencing, it is likely that the acute inhibitory effects of Kir2.1 reflect the adult-specific expression

pattern of this line. However, we cannot rule out the possibility that the phenotype of these flies arises in part due to secondary effects associated with developmental silencing in an expanded population of clock cells, including sLNvs, due to the lack of Pdf-GAL80 suppression during early developmental stages.

We also found that both feeding and locomotor activity rhythms were degraded in the face of electrical silencing of sLNv clock neurons with SS00681-sGAL4 (Figure 3C and K), although the impact of silencing appeared to be muted compared to molecular clock elimination in these cells. Nearly all SS00681>Kir2.1^{eGFP} flies retained rhythmic feeding and activity, and this was associated with an overall smaller magnitude decrease in rhythm strength compared to that observed following molecular clock elimination in sLNv cells (Figure 3C and Table S2). This is unexpected given that neuronal silencing should have more profound functional consequences than clock abrogation, which would still leave the cells intact and able to communicate with downstream targets. It is possible that split GAL4 lines such as SS00681-sGAL4 drive relatively weak expression of Kir2.1, conferring incomplete silencing. This issue would be less acute in our clock ablation experiments given the much higher sensitivity of the CRISPR approach to GAL4 expression levels.

We were unable to test the consequences of LNd neuronal silencing using the LNd-GAL4 line, as LNd>Kir2.1^{eGFP} flies did not survive to adulthood. However, we were able to test the effect of electrical silencing with the more restricted MB122B-GAL4 line. Here, we saw a significant reduction of feeding rhythm strength with no corresponding change in the power of activity rhythms (Figure 2D and L; Table S2), though we note that the reduction in feeding rhythm power was very minor, with experimental flies achieving ~85% of control values. Despite the apparent differential effect on the strength of feeding and activity rhythms, eduction analysis

demonstrated a moderate flattening of the mean waveforms of both activity and feeding behavior (Figure 2H and P).

Together with the experiments discussed above, these results show drastic impacts of eliminating molecular clock function or neuronal activity broadly across the clock network or selectively within subpopulations of lateral clock neurons. These manipulations concomitantly affected multiple circadian outputs including feeding and locomotor activity, demonstrating that these distinct behavioral outputs rely on largely overlapping neuronal circuitry within the lateral cells of the clock network.

Changes in total activity and feeding associated with lateral clock neuron manipulations

In addition to monitoring for circadian patterns of activity and feeding, we also used the DAM and FLIC assays to assess for overall changes in the total amount of activity, measured as the mean number of DAM infrared beam breaks per minute over the course of the experiment, and total feeding time, measured as the mean duration of feeding in minutes per day. Interestingly, we found that *tim*^{CRISPR} flies exhibited a general reduction in both activity and feeding regardless of the GAL4 driver used to induce CRISPR expression (Figure S2A-J). This was not true of the *per*^{CRISPR} line, which often gave results indistinguishable from those obtained with control *acp*^{CRISPR} flies (Figure S2A-J). In fact, we found that CRISPR-mediated clock abrogation with most lateral clock neuron expressing GAL4 lines did not meaningfully impact total activity or feeding. An exception to this lack of effect was the SS00681-sGAL4 line, which showed significant reductions in both total activity and feeding duration when used to drive CRISPR constructs targeting either the *per* or *tim* genes (Figure S2C and H). We also saw that molecular clock abrogation with the MB122B-sGAL4 driver selectively reduced total feeding duration without altering activity amounts (Figure S2E and J). This is consistent with the selective effect of this same manipulation on the power of feeding rhythms (Figure 2E and O).

Genetic silencing of lateral clock neurons produced more profound effects on total activity and feeding compared to CRISPR-mediated molecular clock elimination in the same cells. For example, silencing of all clock neurons with Clk856-GAL4 strongly reduced the magnitude of both activity and feeding (Figure S2K and O), in contrast to the lack of effect on the same measures when this line was used in CRISPR experiments (Figure S2A and F). Interestingly, total activity levels were altered in the face of electrical silencing induced with Clk856-GAL4;Pdf-GAL80, SS00681-sGAL4 and MB122B-sGAL4, but this was not associated with a change in total feeding duration (Figure S2L-N and P-R), highlighting the potential for differential regulation of these two behavioral outputs.

DN1p clock neuron manipulations alter the temporal distribution of feeding and activity without substantially altering rhythm strength

Following our manipulations of lateral neurons, we focused our attention on the dorsal clock neurons, which are a heterogenous group that can be distinguished based on their location, size and neurochemistry (Ma et al., 2021; Reinhard et al., 2022). As compared to lateral neurons, they have been less well studied and functionally characterized, and their role in feeding rhythms remains unexplored. We started by targeting the posterior DN1 (DN1p) population, which consists of ~15 clock neurons per hemisphere. We used 3 different GAL4 lines that drive expression in partially overlapping subsets of these neurons. InSITE911-GAL4 labels all 15 DN1ps, although this line has additional expression in a number of non-clock central brain neurons as well as photoreceptor cells (Figure S1F) (Nettnin et al., 2021). Clk4.1-GAL4 (L. Zhang et al., 2010) is more restricted within the nervous system, showing exclusive expression in ~8-10 DN1p neurons per central brain hemisphere (Figure S1G), but this line also labels many non-neuronal cells in peripheral tissues. Finally, SS00781-sGAL4 (Guo et al., 2017) is expressed in ~6 DN1p cells per hemisphere, in addition to a small handful of non-clock neurons

(Figure S1H). Notably, the effect of driving *per*^{CRISPR} with these lines produced selective reductions in the number of PER+ DN1 cells, and the magnitude of these effects are consistent with the relative number of DN1 cells labeled by each line (Figure 1K and Table 1).

Elimination of the molecular clock in DN1p cells resulted in only minimal and inconsistent effects on the strength of locomotor activity and feeding rhythms (Figure 4A-C and K-M). Nevertheless, these manipulations strongly altered the temporal profile of locomotor activity and feeding across the day (Figure 4F-H and P-R). In control flies, locomotor activity and feeding behavior start at relatively low values in the early subjective morning and steadily ramp up over the next several hours, peaking in the late subjective day before dropping following the onset of subjective night. In contrast, flies in which the molecular clock is removed from DN1p cells exhibit a flattening of these normally dynamic oscillations across the subjective day such that activity and feeding are elevated in the early subjective morning and plateau through the rest of the subjective day, exhibiting a reduced magnitude of the normal subjective evening peak (Figure 4F-H and P-R). These flies also showed increased activity levels compared to controls at the end of the subjective night (Figure 4F-H). These changes were remarkably consistent across all 3 DN1p lines tested, albeit with reduced severity when manipulations were induced with SS00781-sGAL4 (Figure 4H and R), potentially because this line targets the smallest subset of DN1p cells among the 3 drivers. Despite these temporal differences compared to controls, loss of DN1p clocks did not substantially alter the total amplitude of activity and feeding changes across the day, which explains why the strength of rhythmicity of these measures was largely retained.

Consistent with our previous findings (Nettnin et al., 2021), we observed a similar flattening of subjective daytime activity following Kir2.1-mediated silencing of DN1p cells (Figure 5E-F), and here we further these observations to show that feeding oscillations are similarly affected

(Figure 5M-N). Thus, DN1p clock cells as a whole appear to function to suppress early morning and drive late afternoon activity and feeding. This contribution depends both on cell-autonomous molecular clock function within these cells as well as preserved neuronal activity. We note that we were unable to test for the effect of silencing in Clk4.1>Kir2.1^{eGFP} flies, which exhibited developmental lethality likely due to non-neuronal expression of this GAL4 line (Nettnin et al., 2021). In total, our DN1p experiments demonstrate that these cells contribute to the distribution of both feeding and activity behavior across the day but are dispensable for the overall circadian regulation of these output behaviors.

In addition to these effects on the pattern of activity across the day, we found that InSITE911-driven Kir2.1 also drastically reduced the rhythm power of locomotor activity to about 50% of control values (Figure 5A). In contrast, there was only a minor and insignificant drop in feeding behavioral rhythms (Figure 5I). This reduction of rhythmicity was not observed following silencing of SS00781-sGAL4 cells. As we have argued previously (Nettnin et al., 2021), the drastic reduction in activity rhythm strength in InSITE911>Kir2.1^{eGFP} flies likely reflects the impact of silencing the non-clock neurons in which this line is expressed (Figure S1F), which may directly regulate locomotor activity. We also found that silencing of InSITE911-GAL4-expressing cells reduced overall activity amount without affecting feeding duration (Figure S3K and O). These results are consistent with the preferential effect of this manipulation on locomotor activity rhythm strength.

Minimal effects produced by DN2 and DN3 clock neuron manipulations

We also conducted experiments in which we selectively targeted the DN2 or DN3 clock cells. Both feeding and activity rhythms were largely intact when we drove *per*- or *tim*-targeting CRISPR constructs in DN2s with Clk9M-GAL4;Pdf-GAL80 (Kaneko et al., 2012), although there was a trend towards a small reduction in rhythm amplitude in these lines (Figure 4D, I, N and S).

Given that this manipulation also non-selectively eliminates molecular clock function in 2 out of 4 sLNvs (Figure 1F and Table 1), the relative maintenance of behavioral rhythms (as compared to the more complete effect of molecular clock ablation simultaneously in all 4 sLNvs with SS00681-sGAL4) demonstrates that only a subset of sLNvs is required to generate rhythmicity (Helfrich-Förster, 1998). Interestingly, we observed a very small but significant reduction in both activity and feeding rhythms following electrical silencing of these cells (Figure 5C and K). This effect could indicate a contribution of DN2 cells to these circadian outputs, though we cannot rule out enduring effects of developmental sLNv silencing, which is expected to occur in this line given the incomplete developmental suppression mediated by Pdf-GAL80.

We also saw subtle effects associated with manipulations using SS00367-sGAL4, which exclusively labels ~2 out of ~35 DN3 clock neurons per brain hemisphere (Figure S1J) (Sun et al., 2022). Interestingly, while activity rhythms were unchanged following molecular clock disruption of DN3s, feeding rhythm power exhibited a small reduction (Figure 4E and O). In contrast, locomotor activity rhythms were selectively depressed following electrical silencing of these cells (Figure 5D and L). We note that these changes are minor, comprising <20% reduction in rhythm strength, suggesting either that the DN3 cells targeted by SS00367-sGAL4 make a minimal contribution to the circadian regulation of these behaviors or that the small differences observed reflect nonspecific experimental variability. However, as SS00367-sGAL4-expressing cells represent a small subset of DN3 cells, further experiments are required to determine the exact contribution of the larger DN3 population to locomotor activity and feeding rhythms.

Also of interest, molecular clock abrogation targeted either to DN2 or DN3 clock cells significantly and selectively reduced the total duration of daily feeding (Figure S3I-J), with no consistent effect on activity levels (Figure S3D-E). In contrast, electrical silencing of these clock

neuron populations induced a nonsignificant trend towards increased feeding (Figure S3Q-R). These results demonstrate that locomotor activity and feeding behavior can be differentially impacted by clock cell manipulations even in cases when overt rhythmicity is unchanged.

Differential control of feeding and activity rhythms by downstream output neurons

Thus far, we have found that clock cell manipulations produce largely similar effects on both locomotor activity and feeding rhythms. This suggests that the central clock coordinately regulates these two associated outputs, perhaps to ensure proper temporal alignment between activity and feeding. We therefore hypothesized that differential circadian regulation of activity and feeding could arise due to distinct output circuitry downstream of the central clock. We have previously identified the *Drosophila* pars intercerebralis as a circadian output node that could serve to connect the central clock to multiple circadian outputs, and showed in particular that PI neurons that express the DH44 peptide are key regulators of circadian locomotor activity rhythms (Cavanaugh et al., 2014; King et al., 2017). DH44 exerts its effects at two receptors, DH44-R1 and DH44-R2 (Johnson et al., 2004, 2005), and mutants for either receptor exhibit reduced activity rhythm strength, consistent with a role for DH44 signaling in the propagation of circadian information across output circuits (King et al., 2017).

Consistent with our previous results (King et al., 2017) we observed a robust reduction in activity rhythm strength in *Dh44-R1* mutant flies such that rhythm power was approximately half that of heterozygous and wildtype controls (Figure 6A). This was associated with a decrease in activity rhythm amplitude that is characterized by a blunted activity peak towards the end of the subjective day and an increase in subjective night activity (Figure 6B). Despite the reduction in activity rhythm strength, *Dh44-R1* mutants retained overt rhythmicity, with nearly all flies exhibiting significant behavioral rhythms as assessed by Lomb-Scargle periodogram (Table S3). *Dh44-R1* mutants have unchanged total activity across the day (Figure S4A), demonstrating

that the reduction in activity rhythm strength is due to a change in the temporal pattern rather than the absolute amount of activity.

In contrast to the nearly 50% reduction in activity rhythm strength, feeding rhythms were more subtly affected in *Dh44-R1* mutants, as we have also reported previously (King et al., 2017). Feeding rhythm power exhibited a small but significant decrease compared to control flies (Figure 6D), with no change in the total duration of feeding (Figure S4B). At the group mean level, the timing of feeding behavior and the amplitude of feeding oscillations exhibited minor alterations in *Dh44-R1* mutants compared to control groups (Figure 6E). Mutant behavior largely tracked with control flies across most of the day, although, as was the case with locomotor activity, mutants showed elevated feeding behavior towards the end of the subjective night. Because data plots that average information across individual flies are sensitive to fly-to-fly differences in intrinsic period, it is possible that the alterations in mean feeding waveforms (as shown in Figure 6B) reflect a desynchronization between otherwise normally rhythmic flies. However, representative individual fly feedograms demonstrate that blunted locomotor activity oscillations occur in single *Dh44-R1* mutants (Figure 6C), consistent with the overall reduced mean rhythm strength of these flies. In contrast, individual *Dh44-R1* mutants retain prominent feeding-fasting cycles (Figure 6F). Thus, although *Dh44-R1* mutations impact both feeding and activity rhythms, the effects are comparatively stronger for locomotor activity, demonstrating a preferential role for DH44-R1-expressing neurons in generating circadian activity rhythms.

Discussion

Despite the recognized importance of feeding rhythms for metabolic health (Bass, 2012), relatively little is known about the circuit mechanisms that drive rhythmic feeding behavior. In *Drosophila*, most circadian research has used locomotor activity as a behavioral endpoint, but recent technological innovations have enabled automated monitoring of feeding behavior on

longer timescales necessary to assess circadian rhythmicity (Murphy et al., 2017; Ro et al., 2014). Using these tools in combination with cell-specific manipulations, we undertook a detailed investigation of the contribution of subsets of neurons within the *Drosophila* central clock network to feeding behavior. In parallel, we determined the consequences of the same manipulations on locomotor activity rhythms, thereby allowing us to delineate how two prominent behavioral outputs are coordinately controlled by the circadian system.

We relied on a growing resource of clock-neuron expressing GAL4 lines to selectively target the majority of central clock network subsets. In many of these cases, specificity is achieved through intersectional approaches such as the split-GAL4 system or the simultaneous use of GAL80 to delimit GAL4 activity (Venken et al., 2011). Importantly, we combined multiple methods to assess GAL4 activity. We first drove expression of UAS-mCD8::GFP (Figure S1), which labels GAL4-expressing cells with a membrane-tethered GFP construct. This confirmed reported expression patterns and suggested that the 10 GAL4 lines we used in our experiments were largely restricted to the cells of interest. However, functional assessment of GAL4 activity through investigation of CRISPR-mediated elimination of the PER protein offered a slightly different picture, particularly for lines that used Pdf-GAL80. We found that CRISPR-mediated clock ablation was not prevented in Pdf-expressing cells in these lines despite effective elimination of mCD8::GFP in the same cells (Figure 1 and Table 1). This suggests that transient per^{CRISPR} expression occurred prior to the onset of GAL80 expression. Interestingly, this effect was selective for some but not all sLNv cells, supporting the results of other recent studies that indicated that this cell population can be further stratified into multiple subsets (Shafer et al., 2022). The expanded impact of our manipulations beyond the targeted cell population constrains inferences that we can make from behavioral assays using these lines. More generally, this demonstrates the need to confirm adult phenotypes when GAL4 expression

patterns may be developmentally dynamic. This is especially true in cases where manipulations confer irreversible effects, such as occurs with CRISPR.

Control groups in our CRISPR experiments consisted of flies in which GAL4 transgenes drove expression of CRISPR constructs targeting the non-circadian *Acp98AB* gene. This strategy allowed us to maintain consistency in the number and location of transgenic insertions across experimental and control flies, which is not achieved in other commonly used control paradigms such as those that involve flies containing either GAL4 or UAS component alone. We believe that the ability to control for genomic location is particularly important in our CRISPR experiments, in which individual flies contained a combination of 3 to 4 transgenic insertions. Of note, both the UAS-Cas9 transgene and components of the split-GAL4 lines that we used in several of our experimental flies are inserted into the attP2 insertion site on the third chromosome, making experimental flies homozygous for genetic insertions at this locus. Our experimental strategy ensured that this was also true of respective control lines. Our strategy also controlled for potential non-specific effects of GAL4 expression or Cas9 activity within targeted cells. Despite these advantages, the absence of control groups containing UAS-CRISPR elements in the absence of a GAL4 driver precluded our ability to account for potential leaky or non-specific effects of these transgenes. To address this issue, we conducted additional experiments in which we compared flies with UAS-CRISPR components targeting the *per*, *tim* or *Acp98AB* genes in the absence of a GAL4 driver. Importantly, we found that all three groups exhibited strong behavioral rhythms that were indistinguishable from one another (Figure S5), consistent with initial reports using these same lines (Delventhal et al., 2019). These results indicate that any GAL4-independent effects of CRISPR transgenes are negligible.

Our results corroborate previous findings of the relative importance of the lateral clock neurons, and especially the sLNvs, in maintaining rhythms of locomotor activity under conditions of

constant darkness (Grima et al., 2004; Helfrich-Förster, 1998; Renn et al., 1999; Stoleru et al., 2004). We also provide evidence in support of our recent assertion that sLNv function alone is not sufficient for these rhythms, which are sensitive to the abrogation of the molecular clock or neuronal silencing either broadly in non-LNv clock cells or restricted to LNd clock neurons (Bulthuis et al., 2019). Interestingly, we observed remarkably similar effects of these same manipulations on feeding behavior, demonstrating that lateral clock neurons do not differentially regulate activity and feeding.

In contrast to the overt reductions in activity rhythm strength associated with lateral clock neuron manipulations, we found that alterations in dorsal clock neurons produced more subtle changes. We observed a particularly striking effect of DN1p manipulations that suggests a role for these cells in partitioning activity across the day rather than in the generation of rhythms per se. Thus, flies lacking molecular clocks or neuronal firing in DN1p neurons retained normal rhythm amplitude but exhibited a flattening of the normally dynamic changes in activity across the subjective day. This is consistent with an output function for these cells within the clock network, with other clock cells, including the lateral clock neurons, acting as core pacemakers. Notably, DN1p molecular clocks can be entrained by inputs from lateral clock neurons (Chatterjee et al., 2018; Stoleru et al., 2005; L. Zhang et al., 2010). DN1p clocks could serve to regulate the rhythmic release of signaling molecules to propagate circadian information to downstream output cell populations, driving or suppressing feeding and activity at specific times of day. In line with this possibility, DN1p clock neurons exhibit strong rhythms of neuronal excitability, which ramps up in the late night and peaks in the early subjective day (Flourakis et al., 2015; Liang et al., 2016). The coherence and timing of these DN1p neuronal activity peaks depend both on intrinsic molecular clock function and on inputs from lateral clock neurons (Liang et al., 2017). We propose that a lack of molecular clock function or a suppression of action potential generation in DN1p clock neurons eliminates these cyclic neuronal firing patterns, affecting the

phase of activity and feeding by eliminating time-of-day specific drive onto output centers. However, overt rhythmicity is retained due to the maintenance of molecular clock function in lateral pacemaker neurons, which can drive rhythmic behaviors through other output pathways that bypass DN1 clock cells (Liang et al., 2019, 2023).

As was the case for lateral neuron interventions, the impact of DN1p manipulations was quite similar across both activity and feeding assays. Thus, with a few minor exceptions, central clock network manipulations similarly affected both activity and feeding behavior. This may in part stem from the fact that feeding and locomotor activity are tightly intertwined processes with interconnected effects on organismal energy balance. The overlapping influence of metabolic demands on these two behaviors could make them difficult to disentangle. For example, manipulations that increase locomotor activity could result in elevated homeostatic drive to feed associated with heightened energy expenditure. Conversely, cyclic feeding could enable and enforce consolidated periods of sleep and wakefulness by ensuring that energy demands are met throughout the prolonged fasting imposed during sleep. This latter possibility is supported by studies showing that starvation increases locomotor activity and suppresses rhythms of locomotor activity and sleep, presumably to enable foraging (Keene et al., 2010; Lee & Park, 2004).

Importantly, however, despite their interactive nature, feeding and locomotor activity are not indissociable, and studies across multiple organisms have indicated that they are under independent circadian control. For example, mutations in the mouse *per1* gene can differentially impact the phasing of locomotor activity and feeding rhythms, causing feeding to become misaligned with the timing of maximum activity and energy expenditure (Liu et al., 2014). Similarly, disruption of molecular clock function within the *Drosophila* fat body, a peripheral metabolic tissue, has been reported to shift the peak phase of feeding rhythms without altering

locomotor activity patterns (K. Xu et al., 2008), and elimination of the metabolic gene, *Gart*, in peripheral *Drosophila* tissues, including the fat body, strongly dampens rhythmicity of feeding behavior while leaving locomotor activity rhythms intact (He et al., 2023). A potential role for adipose tissue in the selective regulation of feeding behavioral rhythms has also been reported in mammals. Disruption of mouse adipocyte clocks, or mutations in a brain-acting adipokine, exclusively disrupt feeding rhythms, leaving locomotor activity rhythms intact (Paschos et al., 2012; Tsang et al., 2020). Uncoupling of activity and feeding rhythms was also observed following ablation of NPY receptor-expressing neurons in the mediobasal hypothalamus (Wiater et al., 2011), a brain region that houses the agouti-related peptide (AgRP)-expressing neurons that have been tied to rhythmic regulation of hunger and feeding (Cedernaes et al., 2019). Indeed, circadian feeding rhythms may arise from cyclic regulation of hunger and appetitive processes. Notably, forced desynchrony studies have demonstrated a daily oscillation of hunger in humans independent of activity cycles (Scheer et al., 2013). In line with this, *Drosophila* exhibit circadian rhythms in gustatory and olfactory neuron responsiveness, which may contribute to cyclic patterns of their proboscis extension reflex, which assesses appetitive drive to feed (Chatterjee et al., 2010; Tanoue et al., 2004).

Together, these studies demonstrate that feeding rhythms can occur independent of locomotor activity rhythms and therefore that they are under de facto circadian regulation rather than simply occurring secondary to sleep-wake cycles. In fact, we commonly found that many of our control flies showed different overall locomotor and feeding rhythm strength. For example, in many of our control *acp*^{CRISPR} flies, we found that feeding rhythms proceeded at much higher amplitude than activity rhythms (compare Figure 2F-J to Figure 2P-T), with non-normalized rhythm power significantly higher for feeding compared to locomotor activity. This evidences a general lack of correlation between the strength of rhythmicity of these two behavioral outputs, supporting the idea that they are controlled by partially independent processes.

In addition to these non-specific background effects, there were two major instances where we observed significant differential impacts of our manipulations. The first was when we used the InSITE911-GAL4 line to silence DN1p cells, which drastically reduced the strength of locomotor activity rhythms (power was reduced by ~50% compared to controls), but had a more subtle effect on feeding rhythms (power was reduced by ~10% compared to controls, a difference that did not quite reach statistical significance). We did not observe this dissociation with other DN1p-targeting GAL4 lines, suggesting that the silencing of non-clock neurons in InSITE911-GAL4 flies directly impacts locomotor activity. Though the effect likely derives from non-circadian neurons, it nevertheless demonstrates that activity changes are not inextricably linked to changes in feeding.

The second case in which we found a dissociation between effects on activity and feeding rhythms was following genetic elimination of the *Dh44-R1* receptor. Activity rhythm strength of *Dh44-R1* was about half that of controls (Figure 7A-B). This effect was similar in magnitude to that produced by silencing sLNv clock cells (Figure 3C and G), highlighting the significance of DH44 signaling for circadian control of locomotor activity. In contrast, we observed a more subtle decrease in feeding rhythm power in these flies. Thus, though *Dh44-R1* mutation impacted both feeding and activity, the effect on activity rhythms was comparatively greater than that on feeding behavior. Despite the reduction in mean activity rhythm strength and amplitude, we note that the *Dh44-R1* phenotype was variable across individual flies such that some exhibited wildtype activity patterns. In addition, the vast majority of these flies retained a degree of behavioral rhythmicity (Table S3). This indicates that circadian control of locomotor behavior must engage multiple parallel output mechanisms. We hypothesize that the same will be true for circadian control of feeding behavior.

Our results contribute to a growing understanding of the mechanisms through which distinct behavioral and physiological outputs are concurrently regulated by the *Drosophila* circadian system (as recently reviewed in Franco et al., 2018). Thus far, circuit-based mechanisms of circadian control have been investigated for several behavioral outputs in addition to locomotor activity and feeding, including eclosion, temperature preference, courtship and mating, and egg laying. Consistent with our current findings, most of these circadian-controlled behaviors involve important or essential contributions from lateral clock neurons, especially under constant environmental conditions, indicating a common role for these clock neurons across a variety behavioral outputs. An exception is the circadian rhythm of egg-laying behavior, which persists following ablation of Pdf-expressing LNv clock cells (Howlader et al., 2006).

Like locomotor activity and feeding, independent control of other circadian output behaviors appears to derive from distinct neuronal circuitry downstream of the lateral clock cells. In some cases, divergent control first emerges in non-clock output cells, as we have described for feeding and locomotor activity regulation. For example, circadian regulation of eclosion relies on a hierarchical organization in which lateral clock neurons transmit output information to non-clock prothoracicotropic hormone (PTTH)-expressing neurons that in turn communicate with cells in the prothoracic gland to regulate the timing of eclosion (Selcho et al., 2017). In other cases, however, dorsal clock neuron populations appear to make unique contributions to specific behavioral outputs. For example, loss of molecular clock function in DN2 neurons preferentially disrupts rhythms of temperature preference, leaving locomotor activity rhythms intact (Kaneko et al., 2012). Likewise, DN1 cell manipulations differentially impact the timing of locomotor activity and male sex-drive rhythms (Fujii et al., 2007, 2017).

In combination with our current results, these studies suggest that the *Drosophila* circadian system can be modeled as a central hub, consisting of essential clock network populations such

as the lateral clock neurons, that connects to dissociable downstream circuits for the control and coordination of distinct behavioral outputs. These downstream circuits could include dorsal clock neurons as well as non-clock output cell populations. Such an organization would achieve robust central clock network control of different behavioral outputs, which would maximize the strong metabolic and organismal benefit conferred by behavioral coordination. At the same time, it would allow for behavioral flexibility and integration with competing organismal demands through distinct connections to downstream output nodes.

Acknowledgements: We thank David Anderson, Tom Clandinin, Fumika Hamada, Paul Hardin, Michael Rosbash, Gerry Rubin, Amita Sehgal, Orie Shafer, Mimi Shirasu-Hiza, and the Bloomington *Drosophila* Stock Center for fly stocks and Amita Sehgal for antisera.

Funding: The authors disclosed receipt of the following financial support for the research, authorship, and/or publication of this article: This work was supported by the Division of Integrative Organismal Systems of the National Science Foundation, CAREER Award 1942167 to D.J.C.

Declaration of Conflicting Interests: The authors declare that there is no conflict of interest.

Allada, R., & Chung, B. Y. (2010). Circadian organization of behavior and physiology in Drosophila. *Annual Review of Physiology*, *72*, 605–624. https://doi.org/10.1146/annurev-physiol-021909-135815

Bahn, J. H., Lee, G., & Park, J. H. (2009). Comparative analysis of Pdf-mediated circadian behaviors between Drosophila melanogaster and D. virilis. *Genetics*, *181*(3), 965–975. https://doi.org/10.1534/genetics.108.099069

Baines, R. A., Uhler, J. P., Thompson, A., Sweeney, S. T., & Bate, M. (2001). Altered electrical properties in Drosophila neurons developing without synaptic transmission. *The Journal of Neuroscience : The Official Journal of the Society for Neuroscience*, *21*(5), 1523–1531.

Barber, A. F., Fong, S. Y., Kolesnik, A., Fetchko, M., & Sehgal, A. (2021). Drosophila clock cells use multiple mechanisms to transmit time-of-day signals in the brain. *Proceedings of the National Academy of Sciences of the United States of America*, *118*(10). https://doi.org/10.1073/pnas.2019826118

Bass, J. (2012). Circadian topology of metabolism. *Nature*, *491*(7424), 348–356. https://doi.org/10.1038/nature11704

Beckwith, E. J., & Ceriani, M. F. (2015). Experimental assessment of the network properties of the Drosophila circadian clock. *The Journal of Comparative Neurology*, *523*(6), 982–996. https://doi.org/10.1002/cne.23728

Brand, A. H., & Perrimon, N. (1993). Targeted gene expression as a means of altering cell fates and generating dominant phenotypes. *Development (Cambridge, England)*, *118*(2), 401–415.

Bulthuis, N., Spontak, K. R., Kleeman, B., & Cavanaugh, D. J. (2019). Neuronal Activity in Non-LNv Clock Cells Is Required to Produce Free-Running Rest:Activity Rhythms in Drosophila. *Journal of Biological Rhythms*, *34*(3), 249–271. https://doi.org/10.1177/0748730419841468

Cavanaugh, D. J., Geratowski, J. D., Wooltorton, J. R. A., Spaethling, J. M., Hector, C. E., Zheng, X., Johnson, E. C., Eberwine, J. H., & Sehgal, A. (2014). Identification of a circadian output circuit for rest: Activity rhythms in drosophila. *Cell*, *157*(3), 689–701. https://doi.org/10.1016/j.cell.2014.02.024

Cedernaes, J., Huang, W., Ramsey, K. M., Waldeck, N., Cheng, L., Marcheva, B., Omura, C., Kobayashi, Y., Peek, C. B., Levine, D. C., Dhir, R., Awatramani, R., Bradfield, C. A., Wang, X. A., Takahashi, J. S., Mokadem, M., Ahima, R. S., & Bass, J. (2019). Transcriptional Basis for Rhythmic Control of Hunger and Metabolism within the AgRP Neuron. *Cell Metabolism*, *29*(5), 1078-1091.e5. https://doi.org/10.1016/j.cmet.2019.01.023

Chatterjee, A., Lamaze, A., De, J., Mena, W., Chélot, E., Martin, B., Hardin, P., Kadener, S., Emery, P., & Rouyer, F. (2018). Reconfiguration of a Multi-oscillator Network by Light in the Drosophila Circadian Clock. *Current Biology*, 1–11. https://doi.org/10.1016/j.cub.2018.04.064

Chatterjee, A., Tanoue, S., Houl, J. H., & Hardin, P. E. (2010). Regulation of gustatory physiology and appetitive behavior by the Drosophila circadian clock. *Current Biology : CB*, *20*(4), 300–309. https://doi.org/10.1016/j.cub.2009.12.055

Delventhal, R., O'Connor, R. M., Pantalia, M. M., Ulgherait, M., Kim, H. X., Basturk, M. K., Canman, J. C., & Shirasu-Hiza, M. (2019). Dissection of central clock function in Drosophila through cell-specific CRISPR-mediated clock gene disruption. *ELife*, *8*. https://doi.org/10.7554/eLife.48308

Díaz, M. M., Schlichting, M., Abruzzi, K. C., Long, X., & Rosbash, M. (2019). Allatostatin-C/AstC-R2 Is a Novel Pathway to Modulate the Circadian Activity Pattern in Drosophila. *Current Biology : CB*, *29*(1), 13-22.e3. https://doi.org/10.1016/j.cub.2018.11.005

Flourakis, M., Kula-Eversole, E., Hutchison, A. L., Han, T. H., Aranda, K., Moose, D. L., White,

K. P., Dinner, A. R., Lear, B. C., Ren, D., Diekman, C. O., Raman, I. M., & Allada, R. (2015). A Conserved Bicycle Model for Circadian Clock Control of Membrane Excitability. *Cell*, *162*(4), 836–848. https://doi.org/10.1016/j.cell.2015.07.036

Franco, D. L., Frenkel, L., & Ceriani, M. F. (2018). The Underlying Genetics of Drosophila Circadian Behaviors. *Physiology (Bethesda, Md.)*, *33*(1), 50–62. https://doi.org/10.1152/physiol.00020.2017

Fujii, S., Emery, P., & Amrein, H. (2017). SIK3-HDAC4 signaling regulates Drosophila circadian male sex drive rhythm via modulating the DN1 clock neurons. *Proceedings of the National Academy of Sciences of the United States of America*, *114*(32), E6669–E6677. https://doi.org/10.1073/pnas.1620483114

Fujii, S., Krishnan, P., Hardin, P., & Amrein, H. (2007). Nocturnal male sex drive in Drosophila. *Current Biology : CB*, *17*(3), 244–251. https://doi.org/10.1016/j.cub.2006.11.049

Fujiwara, Y., Hermann-Luibl, C., Katsura, M., Sekiguchi, M., Ida, T., Helfrich-Forster, C., & Yoshii, T. (2018). The CCHamide1 Neuropeptide Expressed in the Anterior Dorsal Neuron 1 Conveys a Circadian Signal to the Ventral Lateral Neurons in Drosophila melanogaster. *Frontiers in Physiology*, *9*, 1276. https://doi.org/10.3389/fphys.2018.01276

Fulgham, C. V, Dreyer, A. P., Nasseri, A., Miller, A. N., Love, J., Martin, M. M., Jabr, D. A., Saurabh, S., & Cavanaugh, D. J. (2021). Central and Peripheral Clock Control of Circadian Feeding Rhythms. *Journal of Biological Rhythms*, *36*(6), 548–566. https://doi.org/10.1177/07487304211045835

Gohl, D. M., Silies, M. A., Gao, X. J., Bhalerao, S., Luongo, F. J., Lin, C.-C., Potter, C. J., & Clandinin, T. R. (2011). A versatile in vivo system for directed dissection of gene expression patterns. *Nature Methods*, *8*(3), 231–237.

Grima, B., Chélot, E., Xia, R., & Rouyer, F. (2004). Morning and evening peaks of activity rely

on different clock neurons of the Drosophila brain. *Nature*, *431*(7010), 869–873. https://doi.org/10.1038/nature02935

Gummadova, J. O., Coutts, G. A., & Glossop, N. R. J. (2009). Analysis of the Drosophila Clock promoter reveals heterogeneity in expression between subgroups of central oscillator cells and identifies a novel enhancer region. *Journal of Biological Rhythms*, *24*(5), 353–367. https://doi.org/10.1177/0748730409343890

Guo, F., Chen, X., & Rosbash, M. (2017). Temporal calcium profiling of specific circadian neurons in freely moving flies. *Proceedings of the National Academy of Sciences of the United States of America*, *114*(41), E8780–E8787. https://doi.org/10.1073/pnas.1706608114

Guo, F., Yu, J., Jung, H. J., Abruzzi, K. C., Luo, W., Griffith, L. C., & Rosbash, M. (2016). Circadian neuron feedback controls the Drosophila sleep–activity profile. *Nature*, *536*(7616), 292–297. https://doi.org/10.1038/nature19097

Hastings, M. H., Maywood, E. S., & Brancaccio, M. (2018). Generation of circadian rhythms in the suprachiasmatic nucleus. *Nature Reviews. Neuroscience*, *19*(8), 453–469. https://doi.org/10.1038/s41583-018-0026-z

He, L., Wu, B., Shi, J., Du, J., & Zhao, Z. (2023). Regulation of feeding and energy homeostasis by clock-mediated Gart in Drosophila. *Cell Reports*, *42*(8), 112912. https://doi.org/10.1016/j.celrep.2023.112912

Helfrich-Förster, C. (1998). Robust circadian rhythmicity of Drosophila melanogaster requires the presence of lateral neurons: A brain-behavioral study of disconnected mutants. *Journal of Comparative Physiology - A Sensory, Neural, and Behavioral Physiology*, *182*(4), 435–453. https://doi.org/10.1007/s003590050192

Howlader, G., Paranjpe, D. A., & Sharma, V. K. (2006). Non-ventral lateral neuron-based, non-

PDF-mediated clocks control circadian egg-laying rhythm in Drosophila melanogaster. *Journal of Biological Rhythms*, *21*(1), 13–20. https://doi.org/10.1177/0748730405282882

Johnson, E. C., Bohn, L. M., & Taghert, P. H. (2004). Drosophila CG8422 encodes a functional diuretic hormone receptor. *The Journal of Experimental Biology*, *207*(Pt 5), 743–748. https://doi.org/10.1242/jeb.00818

Johnson, E. C., Shafer, O. T., Trigg, J. S., Park, J., Schooley, D. A., Dow, J. A., & Taghert, P. H. (2005). A novel diuretic hormone receptor in Drosophila: evidence for conservation of CGRP signaling. *The Journal of Experimental Biology*, *208*(Pt 7), 1239–1246. https://doi.org/10.1242/jeb.01529

Kaneko, H., Head, L. M., Ling, J., Tang, X., Liu, Y., Hardin, P. E., Emery, P., & Hamada, F. N. (2012). Circadian rhythm of temperature preference and its neural control in Drosophila. *Current Biology*, *22*(19), 1851–1857. https://doi.org/10.1016/j.cub.2012.08.006

Keene, A. C., Duboué, E. R., McDonald, D. M., Dus, M., Suh, G. S. B., Waddell, S., & Blau, J. (2010). Clock and cycle limit starvation-induced sleep loss in Drosophila. *Current Biology : CB*, *20*(13), 1209–1215. https://doi.org/10.1016/j.cub.2010.05.029

King, A. N., Barber, A. F., Smith, A. E., Dreyer, A. P., Sitaraman, D., Nitabach, M. N., Cavanaugh, D. J., & Sehgal, A. (2017). A Peptidergic Circuit Links the Circadian Clock to Locomotor Activity. *Current Biology : CB*, *27*(13), 1915-1927.e5. https://doi.org/10.1016/j.cub.2017.05.089

King, A. N., & Sehgal, A. (2020). Molecular and circuit mechanisms mediating circadian clock output in the Drosophila brain. *The European Journal of Neuroscience*, *51*(1), 268–281. https://doi.org/10.1111/ejn.14092

Lee, G., & Park, J. H. (2004). Hemolymph sugar homeostasis and starvation-induced hyperactivity affected by genetic manipulations of the adipokinetic hormone-encoding

gene in Drosophila melanogaster. *Genetics*, *167*(1), 311–323. https://doi.org/10.1534/genetics.167.1.311

Liang, X., Ho, M. C. W., Zhang, Y., Li, Y., Wu, M. N., Holy, T. E., & Taghert, P. H. (2019). Morning and Evening Circadian Pacemakers Independently Drive Premotor Centers via a Specific Dopamine Relay. *Neuron*, *102*(4), 843-857.e4. https://doi.org/10.1016/j.neuron.2019.03.028

Liang, X., Holy, T. E., & Taghert, P. H. (2016). Synchronous Drosophila circadian pacemakers display nonsynchronous Ca2+ rhythms in vivo. *Science*, *351*(6276), 976–981.

Liang, X., Holy, T. E., & Taghert, P. H. (2017). A Series of Suppressive Signals within the Drosophila Circadian Neural Circuit Generates Sequential Daily Outputs. *Neuron*, *94*(6), 1173-1189.e4. https://doi.org/10.1016/j.neuron.2017.05.007

Liang, X., Holy, T. E., & Taghert, P. H. (2023). Polyphasic circadian neural circuits drive differential activities in multiple downstream rhythmic centers. *Current Biology : CB*, *33*(2), 351-363.e3. https://doi.org/10.1016/j.cub.2022.12.025

Liu, Z., Huang, M., Wu, X., Shi, G., Xing, L., Dong, Z., Qu, Z., Yan, J., Yang, L., Panda, S., & Xu, Y. (2014). PER1 phosphorylation specifies feeding rhythm in mice. *Cell Reports*, *7*(5), 1509–1520. https://doi.org/10.1016/j.celrep.2014.04.032

Logan, R. W., & McClung, C. A. (2019). Rhythms of life: circadian disruption and brain disorders across the lifespan. *Nature Reviews. Neuroscience*, *20*(1), 49–65. https://doi.org/10.1038/s41583-018-0088-y

Ma, D., Przybylski, D., Abruzzi, K. C., Schlichting, M., Li, Q., Long, X., & Rosbash, M. (2021). A transcriptomic taxonomy of Drosophila circadian neurons around the clock. *ELife*, *10*. https://doi.org/10.7554/eLife.63056

Murphy, K. R., Park, J. H., Huber, R., & Ja, W. W. (2017). Simultaneous measurement of sleep

and feeding in individual Drosophila. *Nature Protocols*, *12*(11), 2355–2366. https://doi.org/10.1038/nprot.2017.096

Nassan, M., & Videnovic, A. (2022). Circadian rhythms in neurodegenerative disorders. *Nature Reviews. Neurology*, *18*(1), 7–24. https://doi.org/10.1038/s41582-021-00577-7

Nettnin, E. A., Sallese, T. R., Nasseri, A., Saurabh, S., & Cavanaugh, D. J. (2021). Dorsal clock neurons in Drosophila sculpt locomotor outputs but are dispensable for circadian activity rhythms. *IScience*, *24*(9), 103001. https://doi.org/10.1016/j.isci.2021.103001

Panda, S. (2016). Circadian physiology of metabolism. *Science (New York, N.Y.)*, *354*(6315), 1008–1015. https://doi.org/10.1126/science.aah4967

Paschos, G. K., Ibrahim, S., Song, W.-L., Kunieda, T., Grant, G., Reyes, T. M., Bradfield, C. A., Vaughan, C. H., Eiden, M., Masoodi, M., Griffin, J. L., Wang, F., Lawson, J. A., & Fitzgerald, G. A. (2012). Obesity in mice with adipocyte-specific deletion of clock component Arntl. *Nature Medicine*, *18*(12), 1768–1777. https://doi.org/10.1038/nm.2979

Patke, A., Young, M. W., & Axelrod, S. (2020). Molecular mechanisms and physiological importance of circadian rhythms. *Nature Reviews. Molecular Cell Biology*, *21*(2), 67–84. https://doi.org/10.1038/s41580-019-0179-2

Picot, M., Cusumano, P., Klarsfeld, A., Ueda, R., & Rouyer, F. (2007). Light Activates Output from Evening Neurons and Inhibits Output from Morning Neurons in the Drosophila Circadian Clock. *PLOS Biology*, *5*(11), e315. https://doi.org/10.1371/journal.pbio.0050315

Potter, G. D. M., Skene, D. J., Arendt, J., Cade, J. E., Grant, P. J., & Hardie, L. J. (2016). Circadian Rhythm and Sleep Disruption: Causes, Metabolic Consequences, and Countermeasures. *Endocrine Reviews*, *37*(6), 584–608. https://doi.org/10.1210/er.2016-1083

Qiao, B., Li, C., Allen, V. W., Shirasu-Hiza, M., & Syed, S. (2018). Automated analysis of long-

term grooming behavior in Drosophila using a k-nearest neighbors classifier. *ELife*, *7*. https://doi.org/10.7554/eLife.34497

Reinhard, N., Schubert, F. K., Bertolini, E., Hagedorn, N., Manoli, G., Sekiguchi, M., Yoshii, T., Rieger, D., & Helfrich-Förster, C. (2022). The Neuronal Circuit of the Dorsal Circadian Clock Neurons in Drosophila melanogaster. *Frontiers in Physiology*, *13*, 886432. https://doi.org/10.3389/fphys.2022.886432

Renn, S. C. ., Park, J. H., Rosbash, M., Hall, J. C., & Taghert, P. H. (1999). A pdf Neuropeptide Gene Mutation and Ablation of PDF Neurons Each Cause Severe Abnormalities of Behavioral Circadian Rhythms in Drosophila. *Cell*, *99*(7), 791–802. https://doi.org/10.1016/S0092-8674(00)81676-1

Ro, J., Harvanek, Z. M., & Pletcher, S. D. (2014). FLIC: high-throughput, continuous analysis of feeding behaviors in Drosophila. *PloS One*, *9*(6), e101107. https://doi.org/10.1371/journal.pone.0101107

Roenneberg, T., & Merrow, M. (2016). The circadian clock and human health. *Current Biology*, *26*(10), R432–R443. https://doi.org/10.1016/j.cub.2016.04.011

Ryder, E., Blows, F., Ashburner, M., Bautista-Llacer, R., Coulson, D., Drummond, J., Webster, J., Gubb, D., Gunton, N., Johnson, G., O'Kane, C. J., Huen, D., Sharma, P., Asztalos, Z., Baisch, H., Schulze, J., Kube, M., Kittlaus, K., Reuter, G., … Russell, S. (2004). The DrosDel collection: a set of P-element insertions for generating custom chromosomal aberrations in Drosophila melanogaster. *Genetics*, *167*(2), 797–813. https://doi.org/10.1534/genetics.104.026658

Sakai, T., & Ishida, N. (2001). Circadian rhythms of female mating activity governed by clock genes in Drosophila. *Proceedings of the National Academy of Sciences of the United States of America*, *98*(16), 9221–9225. https://doi.org/10.1073/pnas.151443298

Scheer, F. A. J. L., Morris, C. J., & Shea, S. A. (2013). The internal circadian clock increases hunger and appetite in the evening independent of food intake and other behaviors. *Obesity (Silver Spring, Md.)*, *21*(3), 421–423. https://doi.org/10.1002/oby.20351

Schlichting, M., Díaz, M. M., Xin, J., & Rosbash, M. (2019). Neuron-specific knockouts indicate the importance of network communication to Drosophila rhythmicity. *ELife*, *8*. https://doi.org/10.7554/eLife.48301

Seay, D. J., & Thummel, C. S. (2011). The circadian clock, light, and cryptochrome regulate feeding and metabolism in Drosophila. *Journal of Biological Rhythms*, *26*(6), 497–506. https://doi.org/10.1177/0748730411420080

Selcho, M., Millán, C., Palacios-Muñoz, A., Ruf, F., Ubillo, L., Chen, J., Bergmann, G., Ito, C., Silva, V., Wegener, C., & Ewer, J. (2017). Central and peripheral clocks are coupled by a neuropeptide pathway in Drosophila. *Nature Communications*, *8*, 15563. https://doi.org/10.1038/ncomms15563

Shafer, O. T., Gutierrez, G. J., Li, K., Mildenhall, A., Spira, D., Marty, J., Lazar, A. A., & Fernandez, M. de la P. (2022). Connectomic analysis of the Drosophila lateral neuron clock cells reveals the synaptic basis of functional pacemaker classes. *ELife*, *11*. https://doi.org/10.7554/eLife.79139

Sletten, T. L., Cappuccio, F. P., Davidson, A. J., Van Cauter, E., Rajaratnam, S. M. W., & Scheer, F. A. J. L. (2020). Health consequences of circadian disruption. In *Sleep* (Vol. 43, Issue 1). https://doi.org/10.1093/sleep/zsz194

Stoleru, D., Peng, Y., Agosto, J., & Rosbash, M. (2004). Coupled oscillators control morning and evening locomotor behaviour of Drosophila. *Nature*, *431*, 862–868. https://doi.org/10.1038/nature02966

Stoleru, D., Peng, Y., Nawathean, P., & Rosbash, M. (2005). A resetting signal between

Drosophila pacemakers synchronizes morning and evening activity. *Nature*, *438*, 238–242. https://doi.org/10.1038/nature04192

Sun, L., Jiang, R. H., Ye, W. J., Rosbash, M., & Guo, F. (2022). Recurrent circadian circuitry regulates central brain activity to maintain sleep. *Neuron*, *110*(13), 2139-2154.e5. https://doi.org/10.1016/j.neuron.2022.04.010

Tanoue, S., Krishnan, P., Krishnan, B., Dryer, S. E., & Hardin, P. E. (2004). Circadian Clocks in Antennal Neurons Are Necessary and Sufficient for Olfaction Rhythms in Drosophila. *Current Biology*, *14*(8), 638–649. https://doi.org/10.1016/J.CUB.2004.04.009

Tataroglu, O., & Emery, P. (2014). Studying circadian rhythms in Drosophila melanogaster. *Methods (San Diego, Calif.)*, *68*(1), 140–150. https://doi.org/10.1016/j.ymeth.2014.01.001

Tsang, A. H., Koch, C. E., Kiehn, J.-T., Schmidt, C. X., & Oster, H. (2020). An adipokine feedback regulating diurnal food intake rhythms in mice. *ELife*, *9*. https://doi.org/10.7554/eLife.55388

Vaze, K. M., & Sharma, V. K. (2013). On the adaptive significance of circadian clocks for their owners. *Chronobiology International*, *30*(4), 413–433. https://doi.org/10.3109/07420528.2012.754457

Venken, K. J. T., Simpson, J. H., & Bellen, H. J. (2011). Genetic manipulation of genes and cells in the nervous system of the fruit fly. *Neuron*, *72*(2), 202–230. https://doi.org/10.1016/j.neuron.2011.09.021

Watanabe, K., Chiu, H., Pfeiffer, B. D., Wong, A. M., Hoopfer, E. D., Rubin, G. M., & Anderson, D. J. (2017). A Circuit Node that Integrates Convergent Input from Neuromodulatory and Social Behavior-Promoting Neurons to Control Aggression in Drosophila. *Neuron*, *95*(5), 1112-1128.e7. https://doi.org/10.1016/j.neuron.2017.08.017

Wen, S., Ma, D., Zhao, M., Xie, L., Wu, Q., Gou, L., Zhu, C., Fan, Y., Wang, H., & Yan, J.

(2020). Spatiotemporal single-cell analysis of gene expression in the mouse suprachiasmatic nucleus. *Nature Neuroscience*, *23*(3), 456–467. https://doi.org/10.1038/s41593-020-0586-x

Wiater, M. F., Mukherjee, S., Li, A.-J., Dinh, T. T., Rooney, E. M., Simasko, S. M., & Ritter, S. (2011). Circadian integration of sleep-wake and feeding requires NPY receptor-expressing neurons in the mediobasal hypothalamus. *American Journal of Physiology. Regulatory, Integrative and Comparative Physiology*, *301*(5), R1569-83. https://doi.org/10.1152/ajpregu.00168.2011

Xu, K., Zheng, X., & Sehgal, A. (2008). Regulation of feeding and metabolism by neuronal and peripheral clocks in Drosophila. *Cell Metabolism*, *8*(4), 289–300. https://doi.org/10.1016/j.cmet.2008.09.006

Xu, P., Berto, S., Kulkarni, A., Jeong, B., Joseph, C., Cox, K. H., Greenberg, M. E., Kim, T.-K., Konopka, G., & Takahashi, J. S. (2021). NPAS4 regulates the transcriptional response of the suprachiasmatic nucleus to light and circadian behavior. *Neuron*, *109*(20), 3268-3282.e6. https://doi.org/10.1016/j.neuron.2021.07.026

Zhang, L., Chung, B. Y., Lear, B. C., Kilman, V. L., Liu, Y., Mahesh, G., Meissner, R. A., Hardin, P. E., & Allada, R. (2010). DN1p Circadian Neurons Coordinate Acute Light and PDF Inputs to Produce Robust Daily Behavior in Drosophila. *Current Biology*, *20*(7), 591–599. https://doi.org/10.1016/j.cub.2010.02.056

Zhang, Y., Liu, Y., Bilodeau-Wentworth, D., Hardin, P. E., & Emery, P. (2010). Light and Temperature Control the Contribution of Specific DN1 Neurons to Drosophila Circadian Behavior. *Current Biology*, *20*(7), 600–605. https://doi.org/10.1016/j.cub.2010.02.044

Figure Legends

Figure 1. Cell-specific, CRISPR-mediated molecular clock abrogation. **A-E**, Representative images are shown of adult brains in which the indicated GAL4 line was used to drive CRISPR constructs targeting the *per* gene. Brains were immunostained for PER (red) and PDF (cyan). Each set of images shows a maximum projection through the dorsal (top) and lateral (bottom) clock cells. **A**, +>*per*^{CRISPR} controls, which contain UAS-guide RNA and UAS-Cas9 constructs in the absence of a GAL4 driver, and thus lack CRISPR gene targeting, show the full complement of PER-expressing clock cells. sLNv, lLNv, LNd, DN1, DN2 and DN3 cells are labeled. **B**, Clk856;Pdf80>*per*^{CRISPR} flies lack PER expression in the vast majority of brain clock cells. Note that despite the Pdf-GAL80, PER expression is retained in only 1 of 4 sLNv cells. **C**, SS00681>*per*^{CRISPR} flies have an exclusive and complete loss of PER expression in sLNv cells. **D**, MB122B>*per*^{CRISPR} flies lack PER expression in 3 of 6 LNd clock neurons. **E**, InSITE911>*per*^{CRISPR} flies have no PER-expressing DN1p clock neurons. **F-L**, violin plots showing the mean number of PER-expressing cells within each of the indicated clock cell populations for each of the indicated genotypes. ****, $p < 0.0001$; ***, $p < 0.001$, ** $p < 0.01$, *, $p < 0.05$ compared to Iso31 controls, Dunn's multiple comparisons test.

Figure 2. Molecular clock abrogation in lateral clock neurons strongly degrades both locomotor activity and feeding rhythms. **A-E**, Graphs show normalized Lomb-Scargle rhythm power for locomotor activity data. Dots represent individual fly data and lines are means ± 95% confidence intervals. **F-J**, Eduction plots show mean activity (in normalized infrared beam breaks/30 min) ± 95% confidence intervals for each 30 min time bin over an average DD day. CT stands for circadian time, with CT0-11.5 corresponding to the subjective day (when lights were on during

pre-experiment entrainment) and CT12-23.5 corresponding to the subjective night (when lights were off during entrainment). **K-O**, Graphs show normalized Lomb-Scargle rhythm power for feeding data, as described for A-E. **P-T**, Eduction plots of mean feeding behavior (in normalized licks/30 min) over time, as described for F-J. For all graphs the indicated GAL4 lines were used to drive *acp*^{CRISPR} (gray), *per*^{CRISPR} (magenta) or *tim*^{CRISPR} (blue). ****, $p < 0.0001$; ***, $p < 0.001$, ** $p < 0.01$, *, $p < 0.05$ compared to *acp*^{CRISPR} controls, Dunnett's T3 multiple comparisons test.

Figure 3. Electrical silencing of lateral clock neurons strongly degrades both locomotor activity and feeding rhythms. **A-D**, Graphs show normalized Lomb-Scargle rhythm power for locomotor activity data. Dots represent individual fly data and lines are means ± 95% confidence intervals. **E-H**, Eduction plots show mean activity (in normalized infrared beam breaks/30 min) ± 95% confidence intervals for each 30 min time bin over an average DD day. CT stands for circadian time, with CT0-11.5 corresponding to the subjective day (when lights were on during pre-experiment entrainment) and CT12-23.5 corresponding to the subjective night (when lights were off during entrainment). **I-L**, Graphs show normalized Lomb-Scargle rhythm power for feeding data, as described for A-D. **M-P**, Eduction plots of mean feeding behavior (in normalized licks/30 min) over time, as described for E-H. Note that LNd>Kir2.1^{eGFP} flies exhibited developmental lethality, precluding analysis of this line. For all graphs the indicated GAL4 lines were used to drive mCherry (gray) or Kir2.1^{eGFP} (green). ****, $p < 0.0001$; ***, $p < 0.001$ compared to mCherry controls, Welch's t-test.

Figure 4. Molecular clock abrogation in DN1p clock neurons alters the temporal distribution of activity and feeding across the day. **A-E**, Graphs show normalized Lomb-Scargle rhythm power for locomotor activity data. Dots represent individual fly data and lines are means ± 95% confidence intervals. **F-J**, Eduction plots show mean activity (in normalized infrared beam breaks/30 min) ± 95% confidence intervals for each 30 min time bin over an average DD day.

CT stands for circadian time, with CT0-11.5 corresponding to the subjective day (when lights were on during pre-experiment entrainment) and CT12-23.5 corresponding to the subjective night (when lights were off during entrainment). **K-O**, Graphs show normalized Lomb-Scargle rhythm power for feeding data, as described for A-E. **P-T**, Eduction plots of mean feeding behavior (in normalized licks/30 min) over time, as described for F-J. For all graphs the indicated GAL4 lines were used to drive *acp*^{CRISPR} (gray), *per*^{CRISPR} (magenta) or *tim*^{CRISPR} (blue). ****, $p < 0.0001$; ***, $p < 0.001$, ** $p < 0.01$, *, $p < 0.05$ compared to *acp*^{CRISPR} controls, Dunnett's T3 multiple comparisons test. Note the flattening of activity and feeding oscillations during the subjective daytime in flies in which InSITE911-GAL4 (F and P) and Clk4.1-GAL4 (G and Q) lines were used to drive *per* and *tim*-targeting CRISPR constructs.

Figure 5. Electrical silencing of DN1p clock neurons alters the temporal distribution of activity and feeding across the day. **A-E**, Graphs show normalized Lomb-Scargle rhythm power for locomotor activity data. Dots represent individual fly data and lines are means ± 95% confidence intervals. **F-J**, Eduction plots show mean activity (in normalized infrared beam breaks/30 min) ± 95% confidence intervals for each 30 min time bin over an average DD day. CT stands for circadian time, with CT0-11.5 corresponding to the subjective day (when lights were on during pre-experiment entrainment) and CT12-23.5 corresponding to the subjective night (when lights were off during entrainment). **K-O**, Graphs show normalized Lomb-Scargle rhythm power for feeding data, as described for A-E. **P-T**, Eduction plots of mean feeding behavior (in normalized licks/30 min) over time, as described for F-J. For all graphs the indicated GAL4 lines were used to drive mCherry (gray) or Kir2.1^{eGFP} (green). ****, $p < 0.0001$; ***, $p < 0.001$, ** $p < 0.01$, *, $p < 0.05$ compared to *acp*^{CRISPR} controls, Welch's t-test. Note the flattening of activity and feeding oscillations during the subjective daytime in flies in InSITE911>Kir2.1^{eGFP} (E and M) and SS007681>Kir2.1^{eGFP} (F and N) flies. Clk4.1>Kir2.1^{eGFP} flies exhibited developmental lethality, precluding analysis of this line.

Figure 6. Selective reduction of locomotor activity rhythm strength in *Dh44-R1* mutants. **A**, Graph shows normalized Lomb-Scargle rhythm power for locomotor activity data demonstrating a reduction in activity rhythm strength in *Dh44-R1* mutants compared to controls. Dots represent individual fly data and lines are means ± 95% confidence intervals. **B**, Eduction plot shows mean activity (in normalized infrared beam breaks/30 min) ± 95% confidence intervals for each 30 min time bin over an average DD day. CT stands for circadian time, with CT0-11.5 corresponding to the subjective day (when lights were on during pre-experiment entrainment) and CT12-23.5 corresponding to the subjective night (when lights were off during entrainment). Note the reduced activity rhythm amplitude in *Dh44-R1* mutants. **C**, Representative individual fly activity records are shown for the indicated genotypes. Locomotor activity in number of infrared beam breaks for each 30 min period is plotted over six days in DD conditions. Graphs are double-plotted with 48 hours of data on each line and the second 24 hours replotted at the start of the next line. Gray and black bars above each plot represent subjective day and night, respectively. **D**, Normalized Lomb-Scargle rhythm power for feeding data, as described for A. **E**, Eduction plot of mean feeding behavior (in normalized licks/30 min) over time, as described for B. **F**, Representative individual fly feeding records are shown for the indicated genotypes. Feeding behavior in number of licks for each 30 min period is plotted over six days in DD conditions as described for C. For all graphs, *Dh44-R1*$^{-/-}$ homozygous mutants are shown in blue, control *Dh44-R1*$^{+/-}$ heterozygous mutants are in brown, and control wildtype (Iso31) flies are in gray. ****, $p < 0.0001$; ** $p < 0.01$, *, $p < 0.05$; ns, not significant, Dunnett's T3 multiple comparisons test.

Figure S1. A library of GAL4 lines to target discrete central clock neuron subsets. Representative maximum project images are shown of adult brains in which the indicated GAL4 line was used to drive UAS-mCD8::GFP. Brains were immunostained for GFP (green) and PER

(magenta). Magnified views of the dorsal and lateral clock neurons are shown above and to the right of full brain images. For each line, a brain schematic depicts the clock neurons labeled by GFP (green circles) and those that are unlabeled (white circles). **A**, Clk856-GAL4 labels nearly all brain clock neurons, except for some DN3 cells. **B**, Clk856-GAL4;Pdf-GAL80 drives GFP expression in most non-LNv clock neurons. **C**, SS00681-sGAL4 exclusively labels sLNv clock cells. **D**, LNd-GAL4 is expressed in all 6 LNd and the 5th sLNv clock neurons, in addition to a handful of non-clock cells throughout the brain. **E**, MB122B-sGAL4 exclusively labels 3 LNd clock neurons and the 5th sLNv in each brain hemisphere. **F**, InSITE911-GAL4 drives GFP expression in all DN1p clock neurons in addition to a few other clusters of non-clock cells. **G**, Clk4.1-GAL4 selectively labels 8-10 DN1p cells per brain hemisphere. **H**, SS00781-sGAL4 marks ~6 DN1p clock neurons per hemisphere in addition to a small number of non-clock cells throughout the brain. **I**, Clk9M-GAL4;Pdf-GAL80 drives GFP expression in 2 DN2 cells per hemisphere. **J**, SS00367-sGAL4 labels 2 of ~35 DN3 clock neurons per hemisphere.

Figure S2. Total activity and feeding for lateral clock neuron manipulations. **A-E**, Graphs show total activity (in DAM infrared beam breaks per min). **F-J**, Graphs show total feeding (in min feeding per day). For A-J, the indicated GAL4 lines were used to drive *acp*^{CRISPR} (gray), *per*^{CRISPR} (magenta) or *tim*^{CRISPR} (blue). Dots represent individual fly data and lines are means ± 95% confidence intervals. ****, $p < 0.0001$; ***, $p < 0.001$, ** $p < 0.01$, *, $p < 0.05$ compared to *acp*^{CRISPR} controls, Dunnett's T3 multiple comparisons test. **K-N**, Graphs show total activity (in DAM infrared beam breaks per min). **O-R**, Graphs show total feeding (in min feeding per day). For K-R, the indicated GAL4 lines were used to drive mCherry (gray) or Kir2.1^{eGFP} (green). Dots represent individual fly data and lines are means ± 95% confidence intervals. ****, $p < 0.0001$; ***, $p < 0.001$, ** $p < 0.01$, *, $p < 0.05$ compared to *acp*^{CRISPR} controls, Welch's t-test. Note that LNd>Kir2.1^{eGFP} flies exhibited developmental lethality, precluding analysis of this line.

Figure S3. Total activity and feeding for dorsal clock neuron manipulations. **A-E**, Graphs show total activity (in DAM infrared beam breaks per min). **F-J**, Graphs show total feeding (in min feeding per day). For A-J, the indicated GAL4 lines were used to drive *acp*^{CRISPR} (gray), *per*^{CRISPR} (magenta) or *tim*^{CRISPR} (blue). Dots represent individual fly data and lines are means ± 95% confidence intervals. ****, $p < 0.0001$; ** $p < 0.01$, *, $p < 0.05$ compared to *acp*^{CRISPR} controls, Dunnett's T3 multiple comparisons test. **K-N**, Graphs show total activity (in DAM infrared beam breaks per min). **O-R**, Graphs show total feeding (in min feeding per day). For K-R, the indicated GAL4 lines were used to drive mCherry (gray) or Kir2.1^{eGFP} (green). Dots represent individual fly data and lines are means ± 95% confidence intervals. ****, $p < 0.0001$; ***, $p < 0.001$, ** $p < 0.01$, *, $p < 0.05$ compared to *acp*^{CRISPR} controls, Welch's t-test. Note that Clk4.1>Kir2.1^{eGFP} flies exhibited developmental lethality, precluding analysis of this line.

Figure S4. Total activity and feeding for *Dh44-R1* mutants. **A**, Total activity (in DAM infrared beam breaks per min). **B**, Total feeding (in min feeding per day). For all graphs, *Dh44-R1*$^{-/-}$ homozygous mutants are shown in blue, control *Dh44-R1*$^{+/-}$ heterozygous mutants are in brown, and control wildtype (Iso31) flies are in gray. Dots represent individual fly data and lines are means ± 95% confidence intervals.

Figure S5. Activity rhythms in flies expressing UAS-CRISPR components in the absence of a GAL4 driver. **A**, Graph shows normalized Lomb-Scargle rhythm power for locomotor activity data for flies expressing UAS-CRISPR transgenes without a corresponding GAL4 driver. Dots represent individual fly data and lines are means ± 95% confidence intervals. Group means are statistically equivalent ($p > 0.519$, Dunnett's T3 multiple comparisons test). **B**, Eduction plot shows mean activity (in normalized infrared beam breaks/30 min) ± 95% confidence intervals for each 30 min time bin over an average DD day. CT stands for circadian time, with CT0-11.5

corresponding to the subjective day (when lights were on during pre-experiment entrainment) and CT12-23.5 corresponding to the subjective night (when lights were off during entrainment).

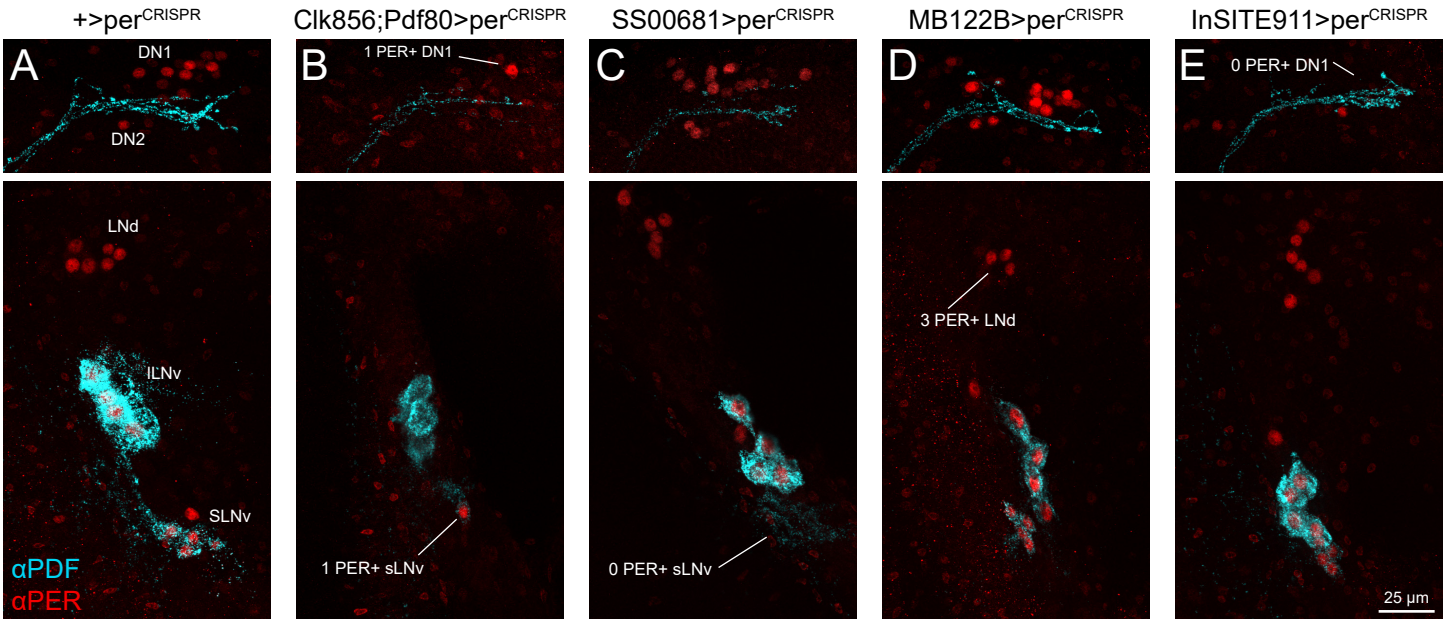
+>per^CRISPR
Clk856;Pdf80>per^CRISPR
SS00681>per^CRISPR
MB122B>per^CRISPR
InSITE911>per^CRISPR
A
DN1
DN2
B
1 PER+ DN1
C
D
E
0 PER+ DN1
LNd
lLNv
SLNv
αPDF
αPER
1 PER+ sLNv
0 PER+ sLNv
3 PER+ LNd
25 μm

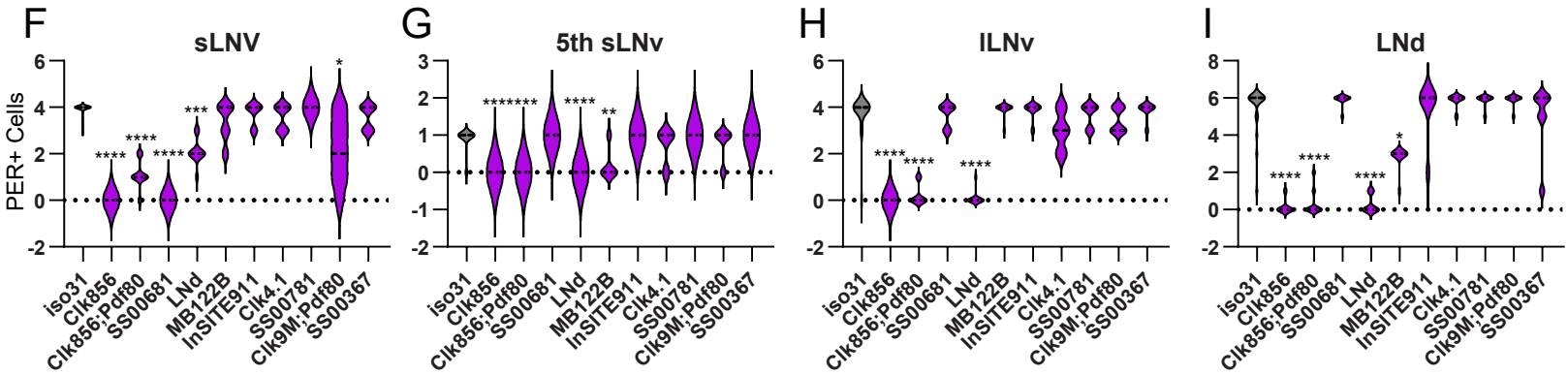
F
sLNV
G
5th sLNv
H
lLNv
I
LNd
PER+ Cells
iso31
Clk856
Clk856;Pdf80
SS00681
LNd
MB122B
InSITE911
Clk4.1
SS00781
Clk9M;Pdf80
SS00367

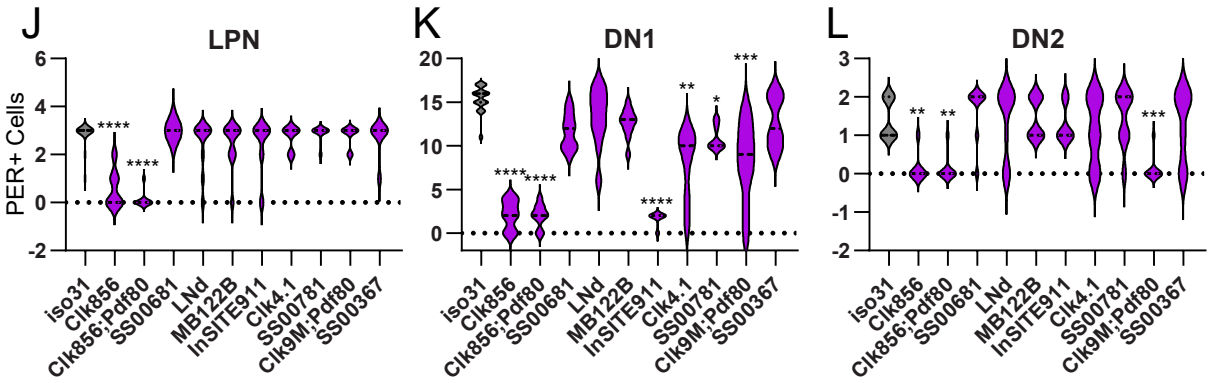
J
LPN
K
DN1
L
DN2
PER+ Cells
iso31
Clk856
Clk856;Pdf80
SS00681
LNd
MB122B
InSITE911
Clk4.1
SS00781
Clk9M;Pdf80
SS00367

Figure 1

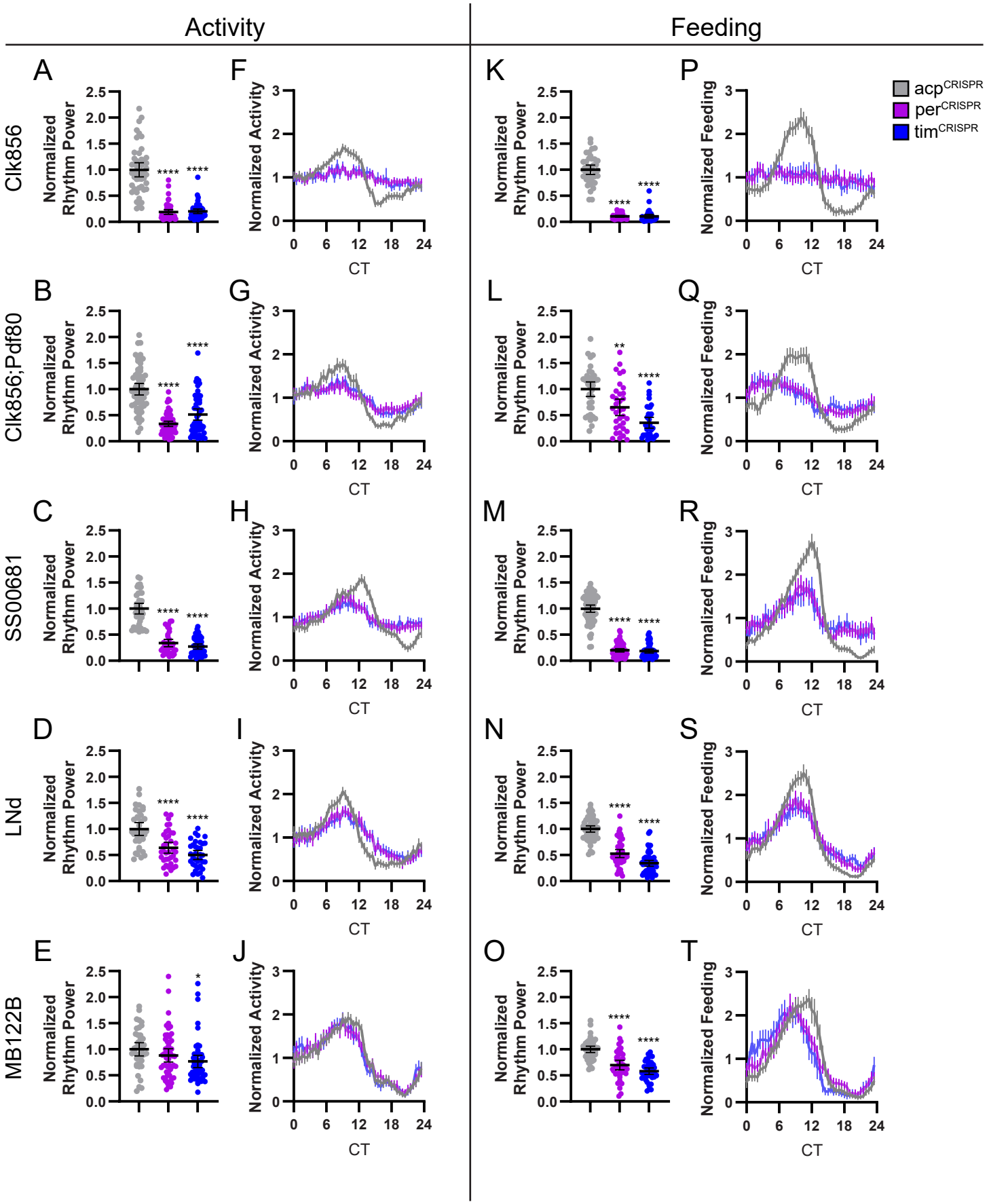
Activity
Feeding
acp^CRISPR
per^CRISPR
tim^CRISPR
Clk856
Clk856;Pdf80
SS00681
LNd
MB122B
A
B
C
D
E
F
G
H
I
J
K
L
M
N
O
P
Q
R
S
T
Normalized Rhythm Power
Normalized Activity
Normalized Feeding
CT
****
**
*

Figure 2

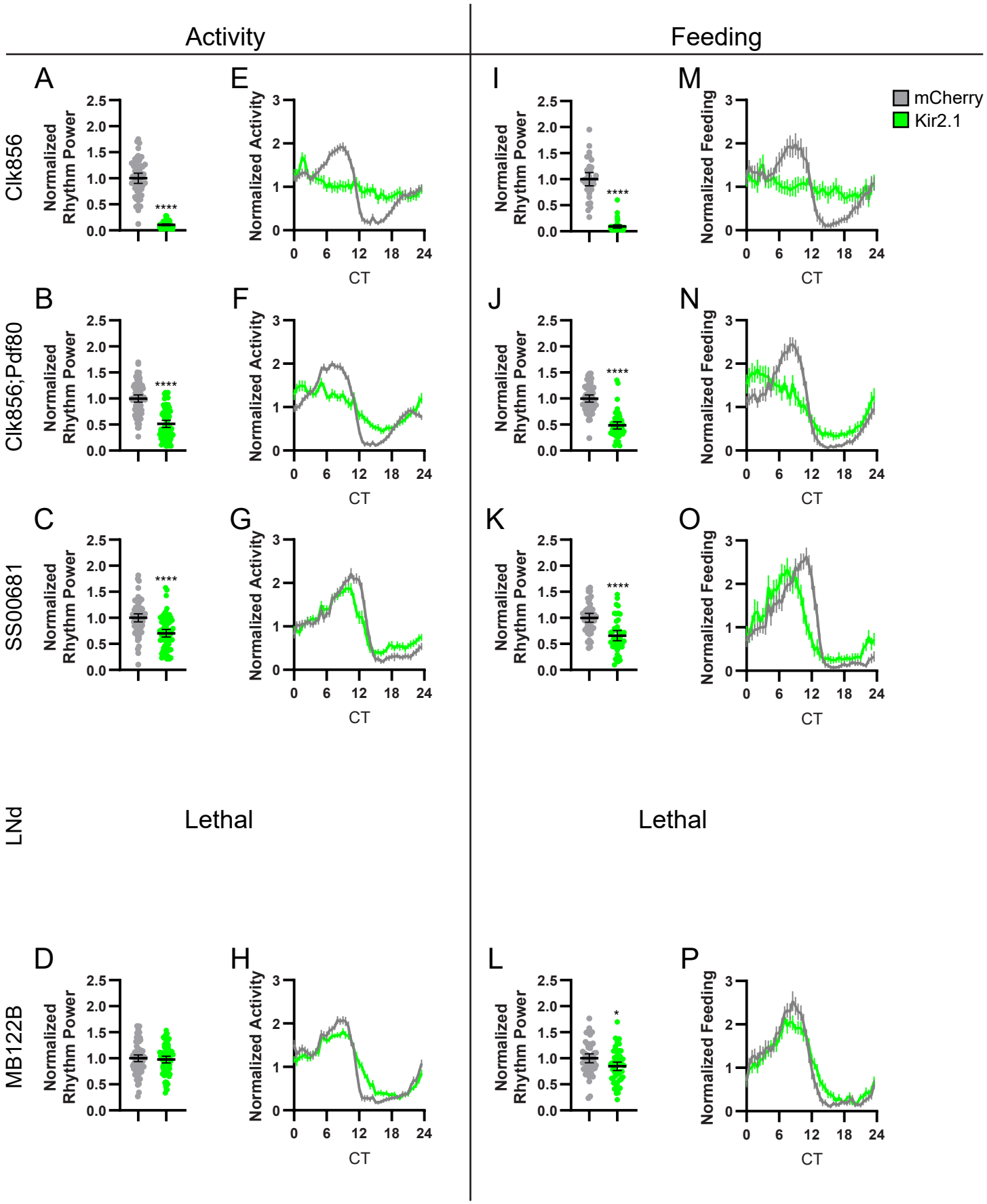
Activity
Feeding
A
B
C
D
E
F
G
H
I
J
K
L
M
N
O
P
Clk856
Clk856;Pdf80
SS00681
MB122B
LNd
Lethal
Lethal
Normalized Rhythm Power
Normalized Activity
Normalized Feeding
CT
****
*
mCherry
Kir2.1

Figure 3

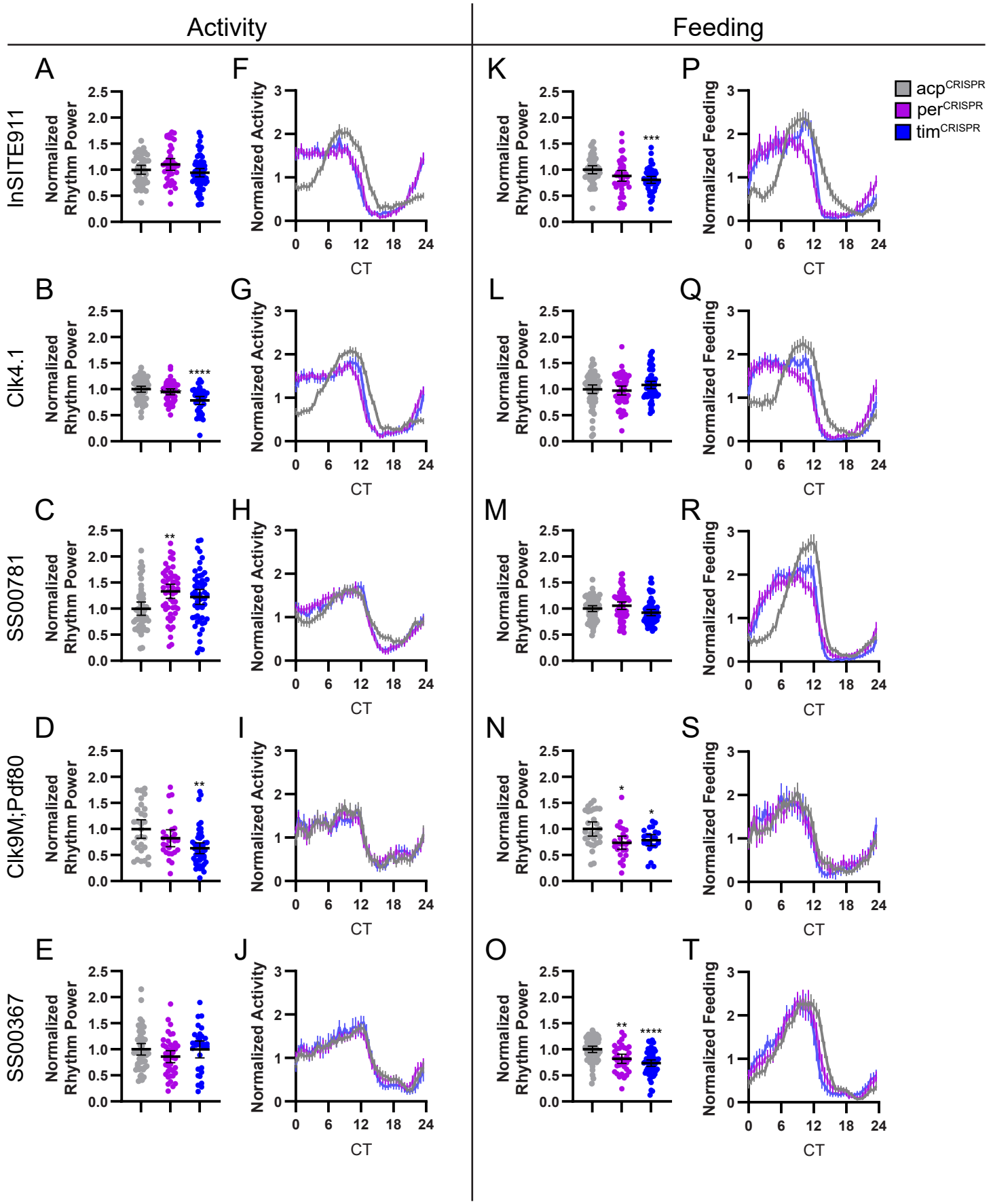
Activity
Feeding
acp^CRISPR
per^CRISPR
tim^CRISPR
lnSITE911
Clk4.1
SS00781
Clk9M;Pdf80
SS00367
A
B
C
D
E
F
G
H
I
J
K
L
M
N
O
P
Q
R
S
T
Normalized Rhythm Power
Normalized Activity
Normalized Feeding
CT
0
6
12
18
24
0.0
0.5
1.0
1.5
2.0
2.5
1
2
3
*
**
***
****

Figure 4

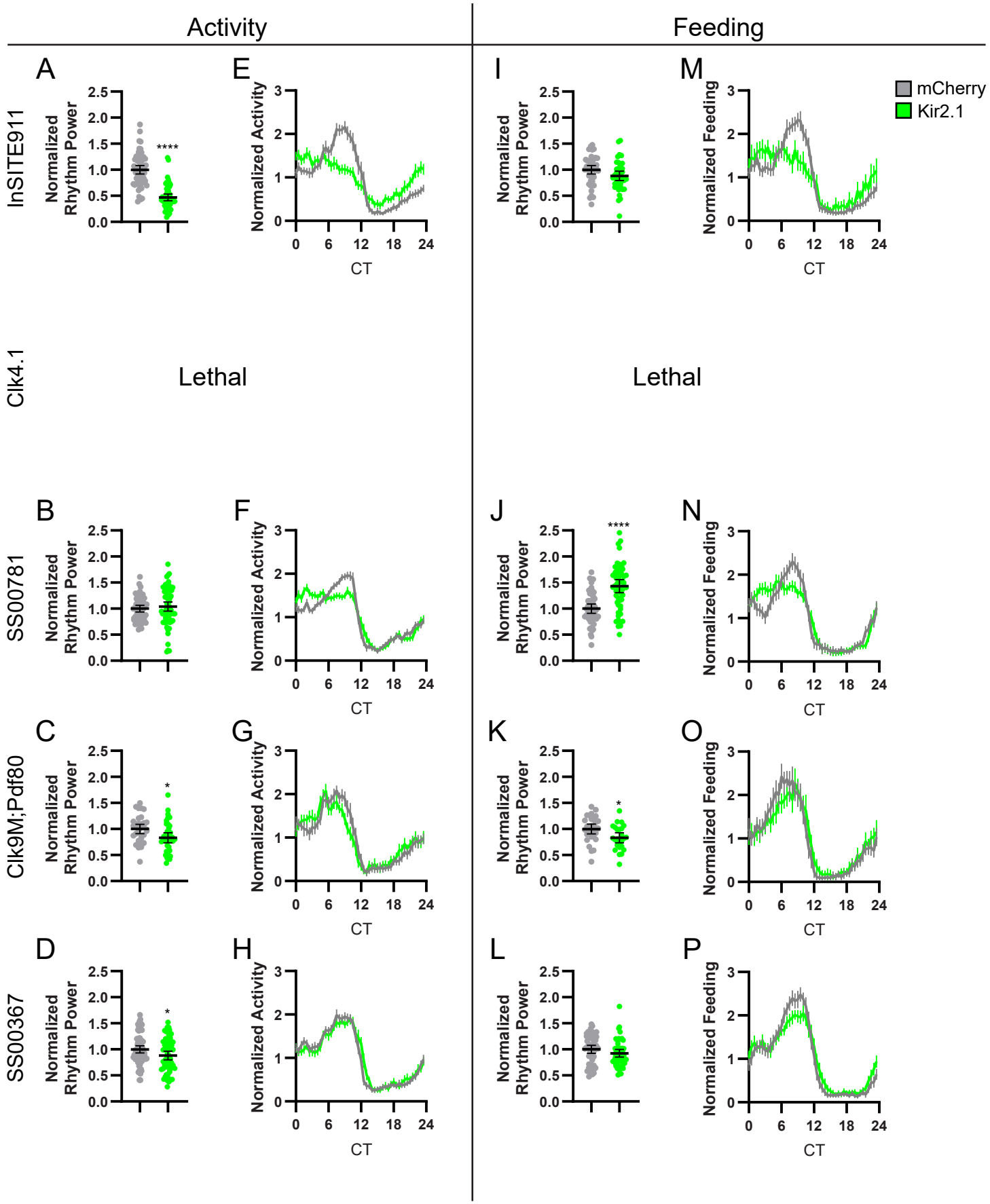
Activity
Feeding
A
E
I
M
mCherry
Kir2.1
InSITE911
Clk4.1
Lethal
Lethal
B
F
J
N
SS00781
C
G
K
O
Clk9M;Pdf80
D
H
L
P
SS00367
Normalized Rhythm Power
Normalized Activity
Normalized Feeding
CT
****
*

Figure 5

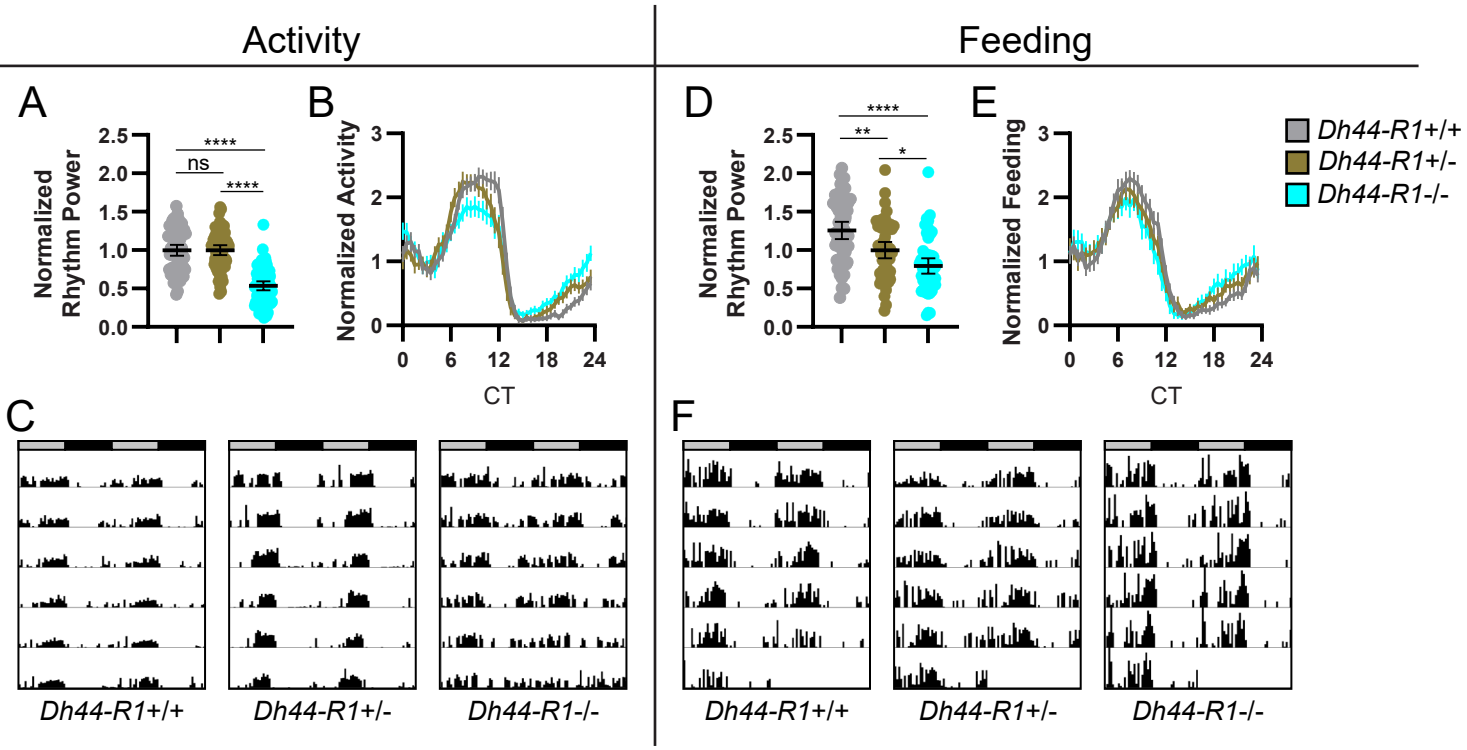
Activity
Feeding
A
B
C
D
E
F
Normalized Rhythm Power
Normalized Activity
Normalized Feeding
CT
ns
****
**
*
Dh44-R1+/+
Dh44-R1+/-
Dh44-R1-/-

Figure 6

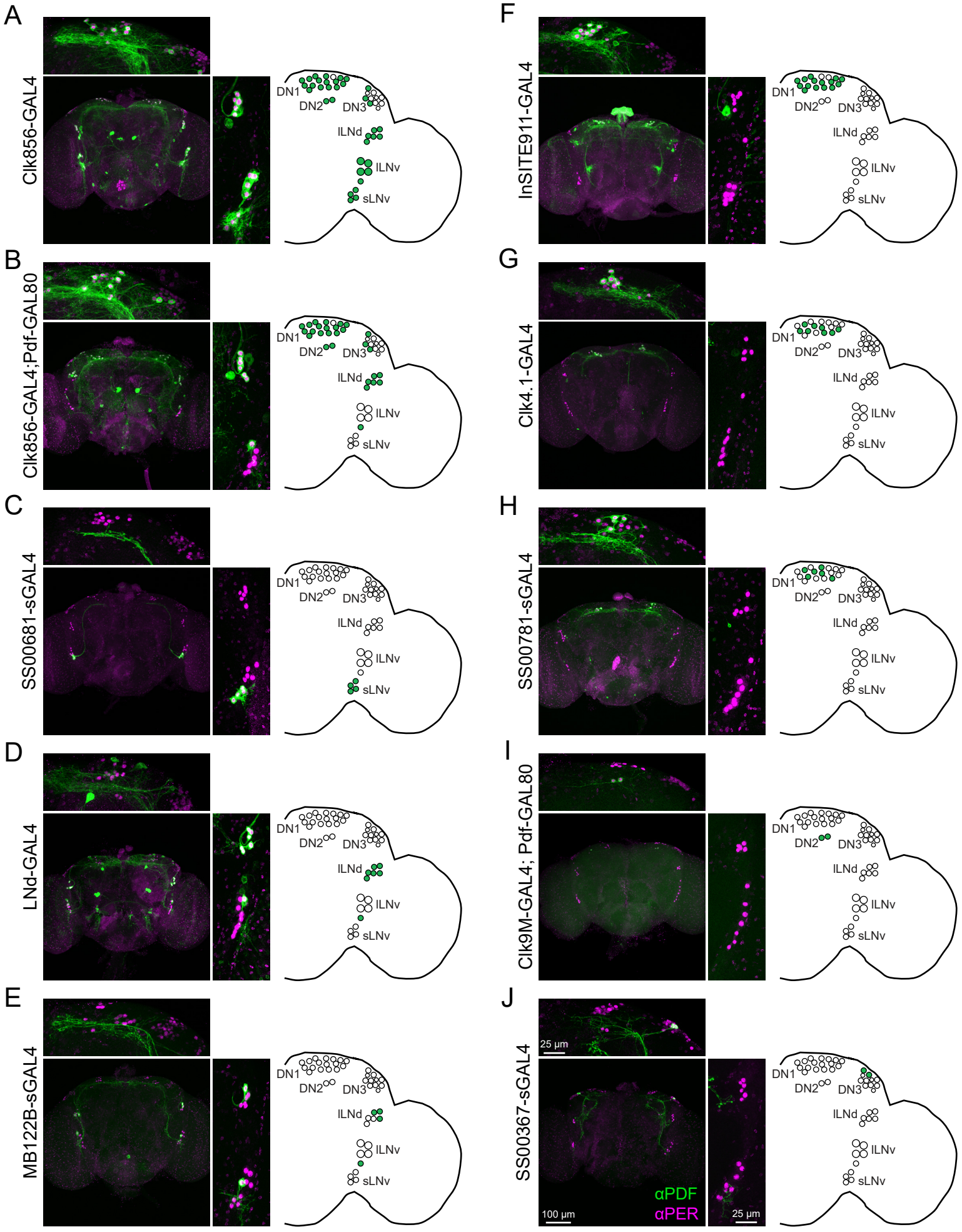
A
Clk856-GAL4
B
Clk856-GAL4;Pdf-GAL80
C
SS00681-sGAL4
D
LNd-GAL4
E
MB122B-sGAL4
F
InSITE911-GAL4
G
Clk4.1-GAL4
H
SS00781-sGAL4
I
Clk9M-GAL4; Pdf-GAL80
J
SS00367-sGAL4
DN1
DN2
DN3
lLNd
lLNv
sLNv
25 µm
100 µm
αPDF
αPER

Figure S1

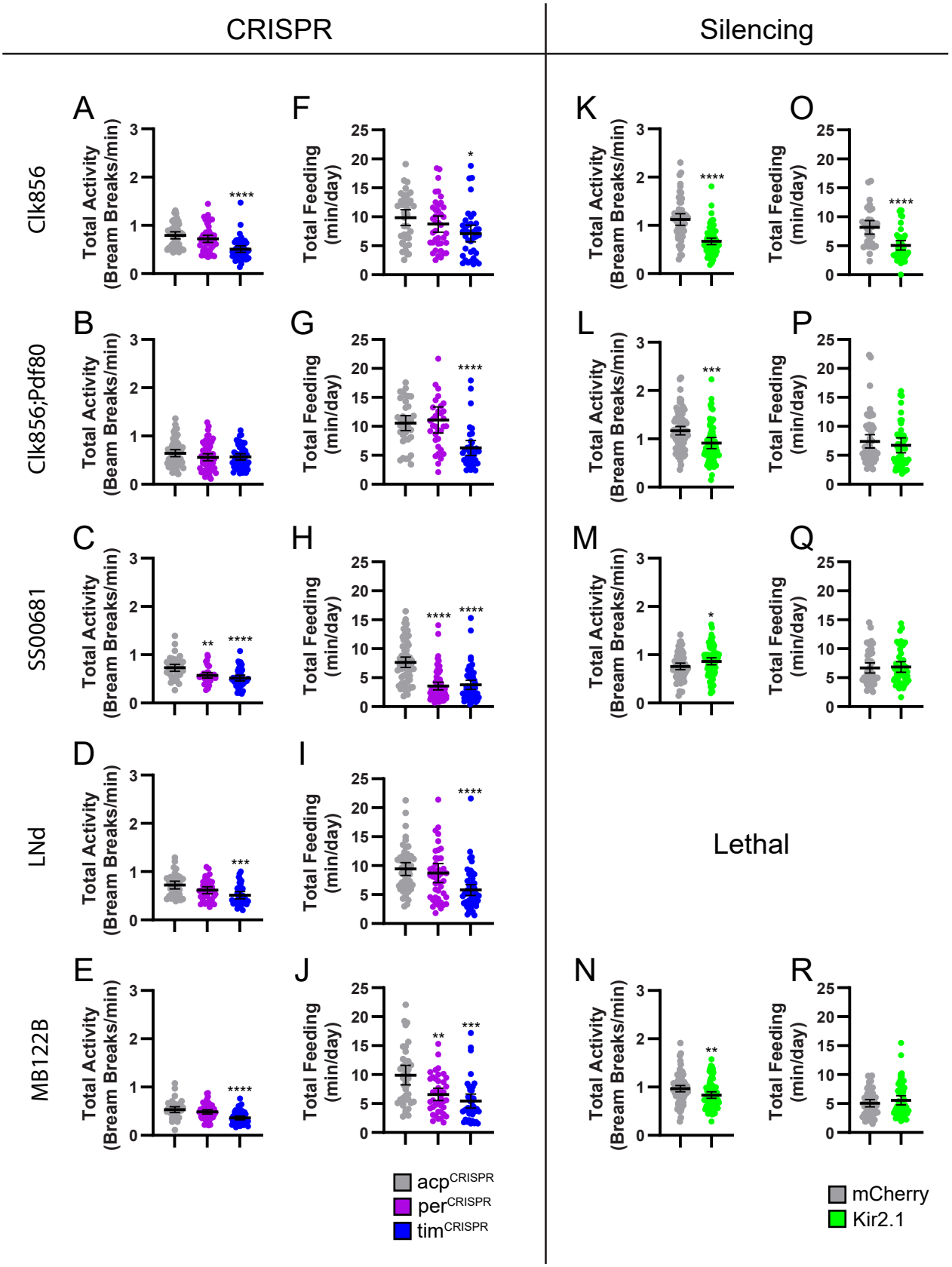
CRISPR
Silencing
Clk856
Clk856;Pdf80
SS00681
LNd
MB122B
A
B
C
D
E
F
G
H
I
J
K
L
M
N
O
P
Q
R
Total Activity (Bream Breaks/min)
Total Feeding (min/day)
Lethal
acp^CRISPR
per^CRISPR
tim^CRISPR
mCherry
Kir2.1

Figure S2

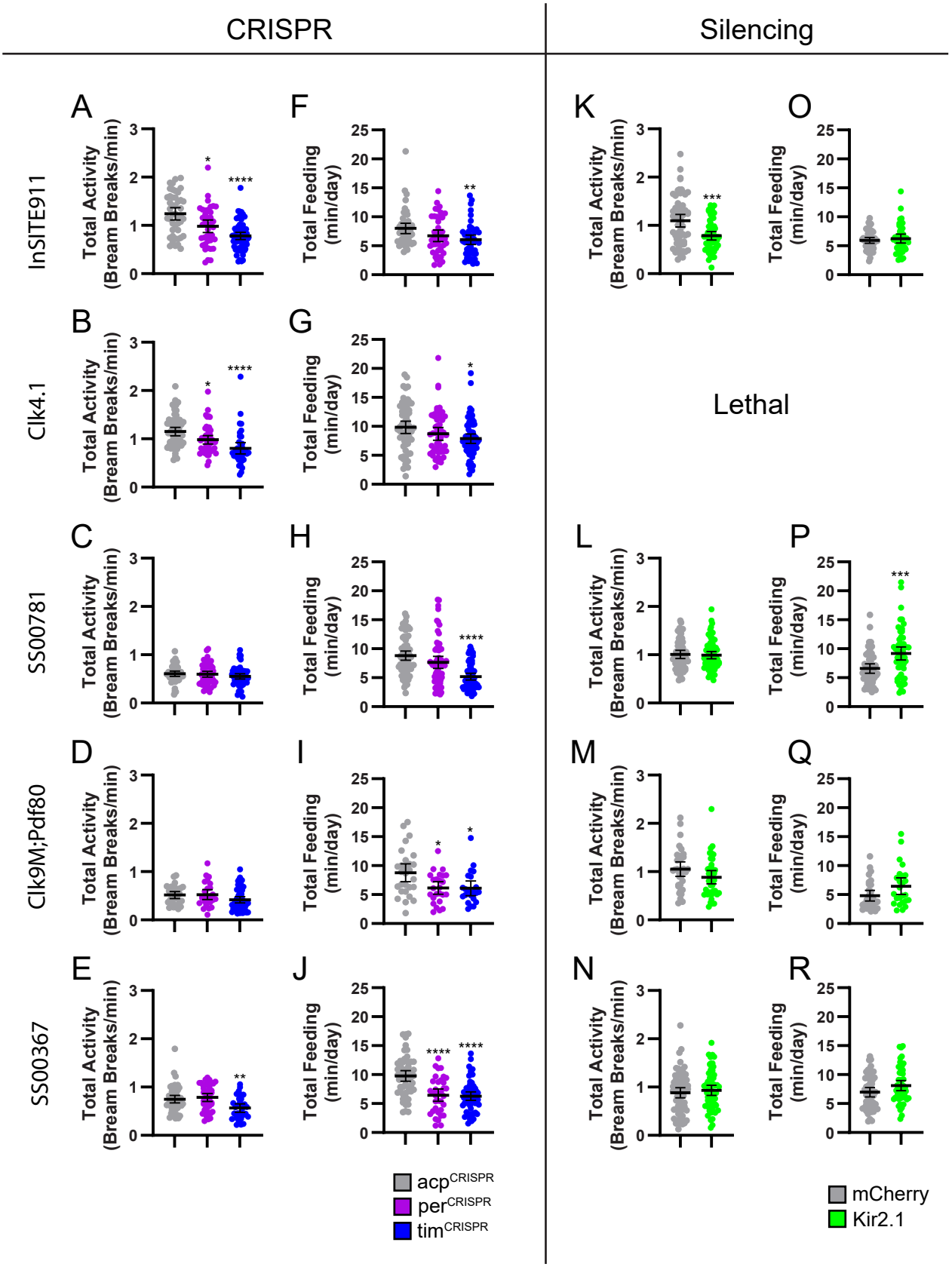
CRISPR
Silencing
InSITE911
Clk4.1
SS00781
Clk9M;Pdf80
SS00367
A
B
C
D
E
F
G
H
I
J
K
L
M
N
O
P
Q
R
Total Activity (Bream Breaks/min)
Total Feeding (min/day)
Lethal
acp^CRISPR
per^CRISPR
tim^CRISPR
mCherry
Kir2.1

Figure S3

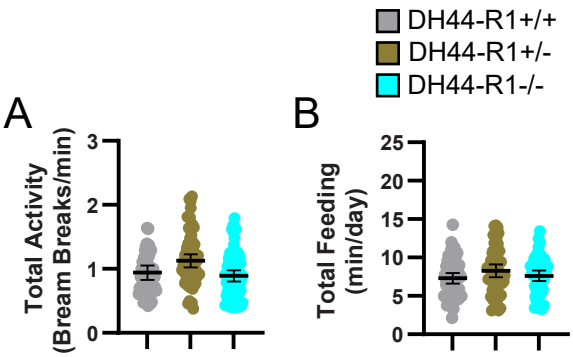
DH44-R1+/+
DH44-R1+/-
DH44-R1-/-
A
Total Activity
(Bream Breaks/min)
3
2
1
0
B
Total Feeding
(min/day)
25
20
15
10
5
0

Figure S4

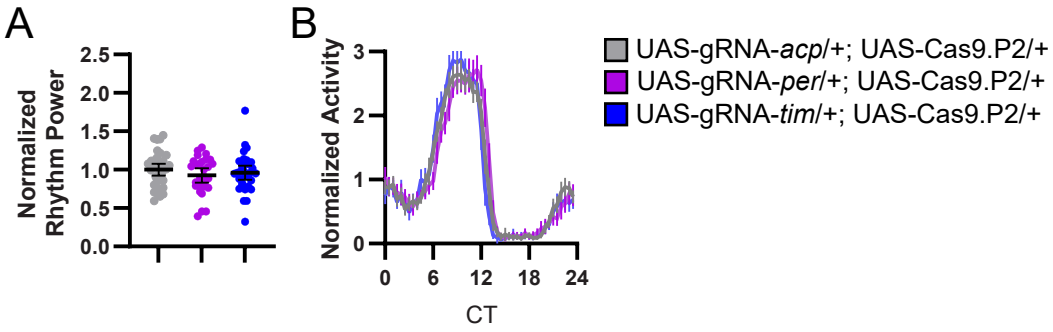
A
Normalized Rhythm Power
2.5
2.0
1.5
1.0
0.5
0.0
B
Normalized Activity
3
2
1
0
0
6
12
18
24
CT
UAS-gRNA-acp/+; UAS-Cas9.P2/+
UAS-gRNA-per/+; UAS-Cas9.P2/+
UAS-gRNA-tim/+; UAS-Cas9.P2/+

Figure S5